Journal of Neuroinflammation

RESEARCH

Open Access

Compromised endothelial Wnt/β-catenin signaling mediates the blood-brain barrier disruption and leads to neuroinflammation in endotoxemia

Xiaowen Huang[1,2,3†], Pengju Wei[1,4†], Cheng Fang[1,4], Min Yu[1,4], Shilun Yang[1,4], Linhui Qiu[1,4], Yu Wang[2,3], Aimin Xu[2,3], Ruby Lai Chong Hoo[2,3] and Junlei Chang[1,4*]

Abstract

The blood-brain barrier (BBB) is a critical interface that maintains the central nervous system homeostasis by controlling the exchange of substances between the blood and the brain. Disruption of the BBB plays a vital role in the development of neuroinflammation and neurological dysfunction in sepsis, but the mechanisms by which the BBB becomes disrupted during sepsis are not well understood. Here, we induced endotoxemia, a major type of sepsis, in mice by intraperitoneal injection of lipopolysaccharide (LPS). LPS acutely increased BBB permeability, activated microglia, and heightened inflammatory responses in brain endothelium and parenchyma. Concurrently, LPS or proinflammatory cytokines activated the NF-κB pathway, inhibiting Wnt/β-catenin signaling in brain endothelial cells in vitro and in vivo. Cell culture study revealed that NF-κB p65 directly interacted with β-catenin to suppress Wnt/β-catenin signaling. Pharmacological NF-κB pathway inhibition restored brain endothelial Wnt/β-catenin signaling activity and mitigated BBB disruption and neuroinflammation in septic mice. Furthermore, genetic or pharmacological activation of brain endothelial Wnt/β-catenin signaling substantially alleviated LPS-induced BBB leakage and neuroinflammation, while endothelial conditional ablation of the Wnt7a/7b co-receptor Gpr124 exacerbated the BBB leakage caused by LPS. Mechanistically, Wnt/β-catenin signaling activation rectified the reduced expression levels of tight junction protein ZO-1 and transcytosis suppressor Mfsd2a in brain endothelial cells of mice with endotoxemia, inhibiting both paracellular and transcellular permeability of the BBB. Our findings demonstrate that endotoxemia-associated systemic inflammation decreases endothelial Wnt/β-catenin signaling through activating NF-κB pathway, resulting in acute BBB disruption and neuroinflammation. Targeting the endothelial Wnt/β-catenin signaling may offer a promising therapeutic strategy for preserving BBB integrity and treating neurological dysfunction in sepsis.

Keywords Endotoxemia, Blood-brain barrier, Neuroinflammation, Wnt/β-catenin signaling, NF-κB pathway

†Xiaowen Huang and Pengju Wei contributed equally to this work.

*Correspondence:
Junlei Chang
jl.chang@siat.ac.cn
[1]Institute of Biomedicine and Biotechnology, Shenzhen Institute of Advanced Technology, Chinese Academy of Sciences, Xueyuan Avenue 1068, Nanshan, Shenzhen, Guangdong 518055, China
[2]Department of Pharmacology and Pharmacy, LKS Faculty of Medicine, The University of Hong Kong, Pokfulam, Hong Kong, China
[3]State Key Laboratory of Pharmacological Biotechnology, LKS Faculty of Medicine, The University of Hong Kong, Pokfulam, Hong Kong, China
[4]The Key Laboratory of Biomedical Imaging Science and System, Chinese Academy of Sciences, Shenzhen, China

© The Author(s) 2024. **Open Access** This article is licensed under a Creative Commons Attribution-NonCommercial-NoDerivatives 4.0 International License, which permits any non-commercial use, sharing, distribution and reproduction in any medium or format, as long as you give appropriate credit to the original author(s) and the source, provide a link to the Creative Commons licence, and indicate if you modified the licensed material. You do not have permission under this licence to share adapted material derived from this article or parts of it. The images or other third party material in this article are included in the article's Creative Commons licence, unless indicated otherwise in a credit line to the material. If material is not included in the article's Creative Commons licence and your intended use is not permitted by statutory regulation or exceeds the permitted use, you will need to obtain permission directly from the copyright holder. To view a copy of this licence, visit http://creativecommons.org/licenses/by-nc-nd/4.0/.

Background

Sepsis is a life-threatening multi-organ dysfunction resulting from dysregulated host immune response to pathogenic infections. According to the Global Burden of Disease Study, 48.9 million people suffer from sepsis each year, and 19.7% of global deaths are related to this disease [1]. Endotoxemia induced by the gram-negative bacterial endotoxin, lipopolysaccharide (LPS), is a major type of sepsis, as gram-negative bacteria infection is the most common infection in patients with sepsis [2, 3]. Sepsis-associated systemic inflammation often causes acute neurological dysfunction with the presentations from mild delirium to deep coma, which is collectively called as sepsis-associated encephalopathy (SAE) [4]. Half of the sepsis patients in the intensive care unit develop SAE and are associated with higher mortality, and many of these patients suffer from long-term cognitive impairments even if surviving from sepsis [5, 6]. However, how SAE is developed in sepsis remains unclear, and there is no effective approach to prevent or treat SAE in clinical practice at present [7].

Although the pathological mechanism of SAE has not been thoroughly elucidated, plenty of studies indicate that neuroinflammation contributes substantially to sepsis-induced neurological dysfunction [8, 9]. The blood-brain barrier (BBB) is the first line to defend against the interference of peripheral inflammatory molecules and cells with the central nervous system (CNS) [10–12]. Disruption of the BBB is found to be related with systemic inflammation in sepsis autopsy on sepsis-related deaths [13]. In sepsis animal model, BBB disruption is always accompanied with the emergence of neuroinflammation, whose manifestations include the activation and hyperplasia of microglia and the elevation of proinflammatory cytokines in brain tissue [8, 9]. Therefore, elucidating how BBB disruption occurs in sepsis will not only increase our understanding of the mechanism of SAE, but also facilitate development of targeted approaches to prevent or treat SAE.

Previous studies have demonstrated that endothelial Wnt/β-catenin signaling plays an essential role in the formation and maintenance of the BBB during development or in adulthood [14–22]. Wnt/β-catenin signaling is highly activated in the CNS endothelial cells (ECs) compared to the non-CNS ECs since early stage of embryogenesis [14, 15]. Genetic mutations of core Wnt/β-catenin signaling components in brain ECs decrease the expressions of tight junction proteins (Claudin-5, Occludin, ZO-1) and Mfsd2a, an omega-3 phospholipid transporter that acts as a potent suppressor of caveolae-mediated transcytosis in CNS ECs [23, 24], thus increasing both the paracellular and transcellular permeability across the BBB [20, 25, 26]. Recent studies including ours showed that compromised endothelial Wnt/β-catenin signaling promotes BBB disruption and aggravates disease outcomes in several CNS disorders, including ischemic stroke [27–30], glioblastoma [27, 31], multiple sclerosis (MS) [32, 33], and Alzheimer's disease (AD) [34]. Furthermore, therapeutic upregulation of endothelial Wnt/β-catenin signaling using engineered Wnt ligands or surrogates effectively alleviates BBB disruption in ischemic stroke and glioblastoma mouse models [35, 36]. Nevertheless, whether endothelial Wnt/β-catenin signaling regulates BBB function during sepsis remain unidentified. Nuclear factor-kappa B (NF-κB) pathway serves as a critical responder to inflammatory stimulations and regulates the expression of various inflammatory genes [37]. The central events in canonical NF-κB pathway activation are the release of p50/p65 dimers from the cytoplasmic inhibition by IκB and the following nuclear translocation of the dimers [38]. Several studies reported a crosstalk between NF-κB and Wnt/β-catenin signaling pathways, and the regulations on each other can be both positively and negatively depending on the cellular types and situations [39–44]. However, little is known about their crosstalk in brain ECs, especially under inflammatory condition.

In the current study, we used lipopolysaccharide (LPS) and proinflammatory factors to imitate the assaults of endotoxin and endotoxin-induced systemic inflammation on brain ECs in mouse models and in vitro cell culture, respectively. Then we showed that brain endothelial Wnt/β-catenin signaling is inhibited by LPS and proinflammatory factors-induced NF-κB activation. Furthermore, we investigated the role of the two signaling pathways played in endotoxemia-associated BBB breakdown with BAY 11-7085 (an inhibitor of NF-κB pathway), Wnt/β-catenin signaling-related genetic mouse models (endothelial-specific activation of β-catenin or knockout of the Wnt7a/7b co-receptor Gpr124), and lithium chloride (LiCl) (an agonist of Wnt/β-catenin signaling [30]). Our study demonstrates that inhibition of brain endothelial Wnt/β-catenin signaling by systemic inflammation-induced NF-κB pathway activation mediates the BBB disruption in endotoxemia, and presents pharmacological activation of endothelial Wnt/β-catenin signaling as a promising therapeutic approach for the treatment of sepsis-induced neurological dysfunction.

Methods

Animals and treatments

C57BL/6J wild-type male mice aged between 8 and 10 weeks were purchased from Vital River Laboratory (Beijing, China). The *Ctnnb1* (the gene encoding β-catenin) exon3 flox mice were generously provided by Dr. Haitao Wu from Beijing Institute of Basic Medical Sciences. The *Ctnnb1* exon3 flox (*Ctnnb1*$^{flox(ex3)}$) mice, *Gpr124* flox mice and *Cdh5-CreER* mice were generated as

previously described [17, 45, 46], and were crossed to generate *Ctnnb1*$^{flox(ex3)/+}$; *Cdh5-CreER*$^{+}$ mice (endothelial β-catenin constitutive activation mice, termed β-cat), *Gpr124*$^{flox/flox}$; *Cdh5-CreER*$^{+}$ mice (endothelial Gpr124 knockout mice, termed Gpr124 ECKO) and their respective wild-type (WT) controls, *Ctnnb1*$^{flox(ex3)/+}$; *Cdh5-CreER*$^{-}$ mice and *Gpr124*$^{flox/flox}$; *Cdh5-CreER*$^{-}$ mice [27]. For induction of β-catenin constitutive activation or Gpr124 endothelial knockout, 7-8-week-old male mice were orally administrated with tamoxifen (Sigma, Cat. #T5648, 2 mg/10 g body weight) in corn oil every other day for 7 days (a total of four times). Mice were allowed to recover from tamoxifen treatment for 2 weeks before further experiments. Animals were housed in 12-hour light and dark cycles in a pathogen free animal facility with free access to food and water. All animal experiments were performed following the "Principles of laboratory animal care" (NIH publication No. 86−23, revised 1985) and in accordance with the National Institutes of Health guidelines for use and care of live animals, and were approved by the Institutional Animal Care and Use Committee of Shenzhen Institute of Advanced Technology, Chinese Academy of Sciences.

Endotoxemia in mice was induced by intraperitoneal injection of lipopolysaccharides (LPS) (from Escherichia coli O55:B5, Sigma, Cat. #L2880, 25 mg/kg body weight). For the inhibition of NF-κB pathway, mice were injected intraperitoneally with the NF-κB inhibitor BAY 11-7085 (5 mg/kg body weight, in 150 μl per mouse) or vehicle control (5% DMSO/saline) at 30 min after LPS injection. For the activation of Wnt/β-catenin signaling, mice were injected intraperitoneally with a Wnt/β-catenin signaling agonist LiCl (3 mmol/kg body weight, in 150 μl per mouse) or vehicle control (saline) at 30 min after LPS injection. For injection of TNF-α, mice were injected intravenously with a low to high dosage of recombinant mouse TNF-α (Sinobiological, Cat. #50349-MNAE, 0.2, 0.3 or 0.4 mg/kg body weight, respectively) or vehicle control (saline) in 100 μl per mouse. All of the animals were included except for those died after induction of endotoxemia and before sacrifice for tissue collection. Mice were randomly distributed to each group. The investigators were blind to treatment/genotype group during the experiment and quantification.

Cell culture

The mouse brain microvascular endothelial cell line bEnd.3 and HEK 293T cells were both obtained from American Type Culture Collection and grown in Dulbecco modified eagle medium (DMEM) supplemented with 10% fetal bovine serum (FBS) and 1% penicillin/streptomycin (P/S). Cells were maintained in a humidified 5% CO2 incubator at 37˚C and routinely passaged when the density of cells was 90–100%.

To knock down *p65* expression in HEK 293T cells, we used small interfering RNA (siRNA) (target sequence is listed in Table S1). To this end, transfection was performed when the density of cells was 30–40%. Lipofectamine RNAi MAX Reagent (Thermo Scientific, Cat. #13778075) and siRNA was diluted in DMEM with no FBS and P/S, respectively. An equal volume of diluted transfection reagent and siRNA was then mixed and incubated at room temperature for 15 min before added to cells. Cells were ready for subsequent experiments 24–48 h after transfection.

TOP-Flash assay

To detect the activity of Wnt/β-catenin signaling, a stable bEnd.3 cell line constructed using TOPFlash firefly luciferase reporter lentivirus (Cignal Lenti TCF/LEF Reporter, QIAGEN) and Renilla luciferase reporter lentivirus as control (Cignal Lenti CMV Renilla Control, QIAGEN) [30], was seeded in 96-well plates. When the density is 80–90%, cells were stimulated with Wnt3a protein (100 ng/ml) and/or specific inflammatory factors including TNF-α, IL-1β, CCL2, IL-17A, IFN-γ and LPS at different concentrations for 24 h. For the treatment of NF-κB inhibitor BAY 11-7085 and Wnt/β-catenin signaling agonist LiCl, cells were stimulated with Wnt3a protein (100 ng/ml) and/or TNF-α (100 ng/ml), IL-1β (10 ng/ml), alongside BAY 11-7085 (10 μM) or LiCl at different concentration for 24 h. TOPFlash firefly and Renilla luciferase activities were measured using the Dual-Luciferase Reporter Assay System (Promega, Cat. #E1910). Wnt/β-catenin signaling activity was presented as TOPFlash firefly/Renilla signal ratio in each group.

RNA isolation and real-time quantitative PCR (RT-qPCR)

bEnd.3 and HEK 293T cells were seeded in 24-well plate and treated in different assays as described above. Total RNA was extracted using the Direct-zol RNA MiniPrep kit (Zymo Research). RNA samples were reversely transcribed using the HiScript III RT SuperMix for qPCR (+gDNA wiper) (Vazyme). RT-qPCR was carried out using LightCycler 96 Real Time PCR system (Roche). DNA expression was calculated using the comparative Ct method normalized to β-actin. The sequences of all primers are shown in Table S2.

Western blotting analysis

Equal amount of protein (20–40 μg) from each sample was separated by performing SDS-PAGE and using 8–10% resolving gels. The resolved proteins were then transferred onto polyvinylidene difluoride membranes (PVDF). Non-fat milk solution (5%) was used to block the membranes for 1 h at room temperature (RT). The membrane was then incubated with primary antibodies (listed in Table S3) at 4˚C overnight and washed five times with

tris-buffered saline/0.1% Triton X-100 (TBST), each time 5 min. Horseradish peroxidase (HRP)-conjugated respective secondary antibodies (listed in Table S3) were added to the membrane, which was then incubated for 1 h at RT and washed again with TBST as mentioned earlier. Chemiluminescent HRP substrate (Millipore; Cat. #WBKLS0500) and GelView 6000 M system (BioLight, GV6000) were used to detect the target protein bands. Target protein levels were qualified by Image J and normalized to GAPDH or Histone-H3.

Bimolecular fluorescence complementation (BiFC) assay

HEK 293T cells were seeded in polylysine-coated round coverslips at the density of 50–60%. When cells became adherent, they were co-transfected with recombinant vector pBiFC-VC155-β-catenin-HA and pBiFC-VN173-p65-FLAG for 12 h, and then treated with or without Wnt3a (100 ng/ml) and TNF-α (100 ng/ml) for 24 h. Cells were fixed with 4% paraformaldehyde, permeabilized with 0.2% Triton-X 100 in PBS, blocked with 5% goat serum, 2% bovine serum albumin (BAS) and 0.05% Triton-X 100 in PBS in turn. Samples were incubated in 4˚C overnight with primary antibody to HA and FLAG (listed in Table S3) in PBS with 1% BAS and 0.05% Triton-X 100. The primary antibody was removed by washing with PBS for 5 min, 3 times. Samples were then incubated at RT with secondary antibody (listed in Table S3) in PBS with 0.05% Triton-X 100. The secondary antibody was removed by washing with PBS for 5 min, 3 times. The samples were mounted in Anti-Fade Reagent with DAPI (Cell Signaling Technology, Cat. #8961S), and imaged with a confocal microscope (Leica, STELLARIS 5). ImageJ software was used to quantify the immunofluorescence signal.

Co-immunoprecipitation (Co-IP)

HEK 293T cell were seeded in 6 cm culture plate at the density of 50-60%. When cells became adherent, they were co-transfected with recombinant vector pcDNA3.1-HA-β-catenin and pcDNA3.1-FLAG-p65 for 12 h, and then treated with or without Wnt3a (100 ng/ml) and TNF-α (100 ng/ml) for 24 h. Whole cell lysates were collected and the protein concentration was determined. 500 μg total protein was used in immunoprecipitation while 50 μg protein used as input. Samples were incubated with HA-magnetic-beads (Thermo Fisher Scientific, Cat. #88836) at 4˚C overnight with slow rotation, and then washed with lysis buffer for 10 min, 3 times using a magnetic grate. Samples were analyzed by SDS-PAGE and Western blotting.

Measurement of Evans Blue Leakage

Mice were retro-orbitally injected with 2% Evans Blue (4 ml/kg body weight) 4 h prior to sacrifice. Mice were deeply anesthetized and transcardially perfused with 20 ml ice-cold PBS to remove the intravascular dye. The brains were dissected and first sectioned into 2 mm coronal slices to take pictures, then homogenized in 1 ml 50% trichloroacetic acid and centrifuged in 12,000 rpm for 15 min. The concentration of Evans Blue in the supernatant was measured by a microplate photometer (ThermoFisher, Multiskan^{TM} FC) at 620 nm. The results were calculated and presented as nanogram (ng) per gram (g) brain tissue according to the standard curve.

Immunofluorescence staining

For immunofluorescence staining of bEnd.3 cells, cells were seeded in round coverslips at the density of 50–60%. When cells became adherent, they were stimulated with Wnt3a protein (100 ng/ml) and/or TNF-α (100 ng/ml) and IL-1β (10 ng/ml) for 24 h. In active β-catenin and NF-κB p65 antibodies staining, cells were fixed with pre-cooled (-20℃) 100% Ethanol or 4% paraformaldehyde (PFA) for 15 min at RT, respectively, followed by permeabilization, blocking, and incubation of primary and secondary antibodies (listed in Table S3) as described above.

For mice tissue staining, mice were deeply anesthetized and transcardiacally perfused with cold PBS as described above. Brain tissues were collected and fixed in 4% PFA for 1 h at RT. Brain tissues were first dehydrated in 15% sucrose at 4 °C overnight, followed by 3–6 h incubation in 30% sucrose at 4 °C. Brain tissues were then embedded in OCT (Sakura, Cat. #4583) for 10–15 min at RT, and stored at -80 °C. To stain PFA fixation-sensitive antibodies (Claudin-5, Occludin, ZO-1, and Active β-catenin, fixation methods are listed in Table S4), the perfused and dissected brain tissues were directly embedded in OCT and snap frozen at -80 °C until being used.

Embedded and frozen tissue were sectioned into 10 μm in thickness on glass slides. Tissue were air dried at RT for 30 min and washed with PBS to remove OCT. Samples were blocked in 10% Goat Serum + 1% BSA + 1% Triton X-100 + 0.05% NaN3 in PBS at RT for 1 h, and then incubated in primary antibodies (listed in Table S3) at 4˚C overnight. Specifically, anti-Mfsd2a antibody was a homemade rabbit polyclonal antibody with an immunogen corresponding to the mouse MFSD2A C-terminus amino acids CSDTDSTELASIL. The specificity has been validated in brain tissues from endothelial β-catenin knockout mice and in HEK 293T cells transiently overexpressing mouse Mfsd2a in our previous study [25]. Excess primary antibody was removed by rinsing with PBS/0.1% Triton X-100 for 10 min 4 times. Afterward, samples were incubated in secondary antibodies (listed in Table S3) at RT for 1 h. Excess secondary antibody was removed by rinsing in PBS/0.1% Triton X-100 for 10 min 4 times. Finally, slides were mounted in Anti-Fade Reagent with DAPI (Cell Signaling Technology, Cat.

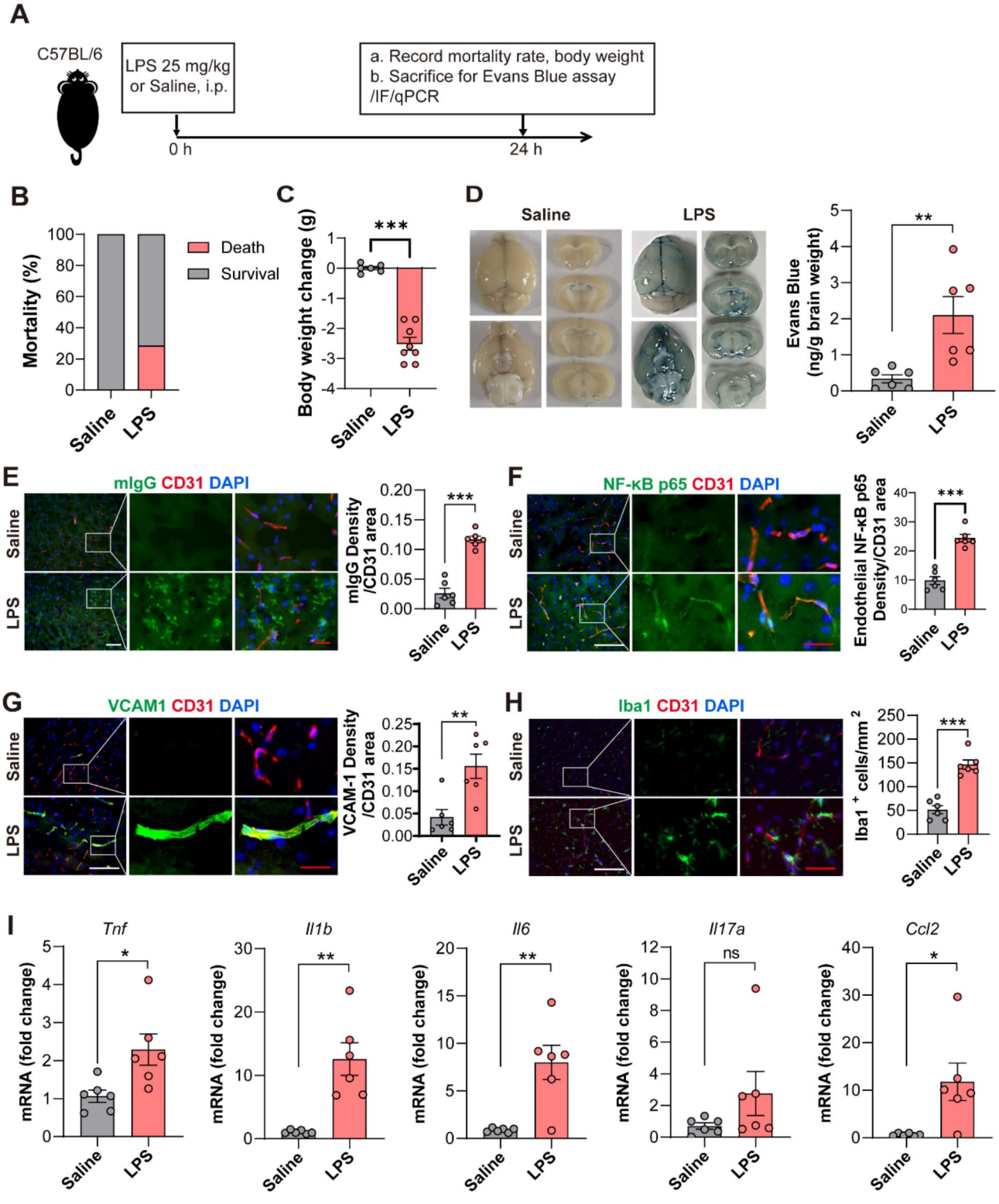

Fig. 1 (See legend on next page.)

(See figure on previous page.)

Fig. 1 LPS causes pervasive BBB leakage and inflammatory responses in brain endothelium and parenchyma. **A**, Schematic illustration of experimental design. Endotoxemia was induced by LPS injection in male C57BL/6J wild-type (WT) mice. **B**, Mortality rate of mice at 24 h following saline ($n=10$ mice) or LPS ($n=14$ mice) treatment. **C**, Body weight change of the mice at 24 h after saline ($n=6$ mice) or LPS ($n=8$ mice) injection. **D**, Representative brain images showing Evans Blue leakage induced by LPS and its quantifications, presented as nanogram dye per gram brain weight (ng/g). **E**, Co-immunofluorescence staining of mouse plasma IgG and CD31 in the brain cortex and its quantifications. **F**, Co-immunofluorescence staining of NF-κB p65 and CD31 in the brain cortex and its quantifications. NF-κB p65 signal in endothelial cells was selectively quantified. **G**, Co-immunofluorescence staining of VCAM1 and CD31 in the brain cortex and its quantifications. **H**, Co-immunofluorescence staining of the microglia marker Iba1 and CD31 in the brain cortex and its quantifications. Iba1$^+$ microglia numbers were normalized to the area of brain tissue. **I**, RT-qPCR analysis of the expression levels of proinflammatory factors *Tnf*, *Il1b*, *Il6*, *Il17a*, and *Ccl2* in the brain cortex tissue (normalized to β-actin). $n=6$ mice per group for **D-I**. White scale bar: 100 μm. Red scale bar: 25 μm. Data are presented as mean ± SEM. ns, no significance, $^*P<0.05$, $^{**}P<0.01$, $^{***}P<0.001$, Student's *t*-test

#8961S). The mouse cerebral cortex region was imaged with a fluorescence microscope (ZEISS, Axio Imager Z2 with ApoTome.2 optical sectioning).

Fluorescence density or area were qualified by Image J. For BBB leakage markers (IgG and albumin), and endothelial specific-expressed targets (tight junctions and transcytosis-associated proteins) staining, the ratio between target protein density and endothelial marker CD31 area was presented. For active β-catenin and NF-κB p65 staining, the ratio between target protein density in CD31-positive endothelial cells and CD 31 area was presented. For Iba1 and GFAP staining, the number of Iba1-positive cells per unit area or GFAP mean density in the cerebral cortex was presented. For bEnd.3 cell staining, the ratio between cell total target protein density and DAPI area was presented as total expression, and the ratio between target protein density in DAPI-positive area and DAPI area was presented as nuclear expression.

FACS sorting of mouse brain endothelial cells

The target gene expression levels of Wnt/β-catenin signaling were detected in FACS-sorted mouse brain ECs, as previously described [27, 47]. Briefly, brain tissue of mice was minced with razor blade thoroughly, and dissociated with Type IV collagenase (400 U/ml, Worthington, Lakewood, NJ), Dispase (1.2 U/ml, Worthington, Lakewood, NJ) and DNase I (32 U/ml, Worthington, Lakewood, NJ) in 6 mL 1× PBS with Ca^{2+} and Mg^{2+} (GIBCO) at 37 °C for 60 min, with gentle trituration every 10 min. 1 ml FBS and 10 ml cold PBS were added to the tubes and samples were filtered through 40 μm cell strainers. After centrifugation at 400 g for 5 min, 4˚C, the pellet was suspended in 10 ml 20% BSA in cold PBS and centrifugated at 1,000 g for 25 min, 4˚C to remove myelin. Pellet was suspended again in 3% FBS in cold PBS for staining. Cells were first blocked with Mouse BD Fc-block (BD Pharmingen, Cat. #553142), then endothelial cells were labeled with PE-Cyanine7 rat anti-mouse CD31, and pericytes were labeled with APC rat anti-mouse PDGFRβ. PE rat anti-mouse CD45 and 7-AAD were added to exclude hematopoietic lineage cells and dead cells, respectively. The detailed information of above antibodies is listed in Table S3. While staining, cells were incubated at 4˚C for 1 h. Cells were washed and CD31$^+$/PDGFRβ$^-$/CD45$^-$/7-AAD$^-$ cells were sorted into 3% FBS in cold PBS with BD FACSAria III (100 μM Nozzle). Sorted cells were centrifuged at 2,000 g for 10 min, 4˚C and suspended in Trizol for RNA extraction and analysis.

Transmission electron microscopy (TEM)

Brain tissues of mice were harvested and immediately fixed by immersion in 2.5% glutaraldehyde/0.1 M PB (pH 7.2) overnight at 4 ℃. The tissue sections were dehydrated in graded ethanol and embedded in epoxy resin. Ultrathin Sect. (80 nm) were then cut from the block surface, collected on copper grids, and stained with uranyl acetate and Reynold's lead citrate. Brain ultrastructure was scanned by transmission electron microscope (Philips CM120).

Statistical analysis

All data were presented as mean±standard error of the mean (SEM). Statistical analysis was performed by GraphPad Prism 8.0. Two-tailed Unpair Student's *t*-test was used in comparison between two groups and One-way ANOVA was used in comparison among more than two groups. Statistical significance was defined as $P < 0.05$.

Results

LPS-induced endotoxemia causes pervasive BBB leakage and inflammatory responses in brain endothelium and parenchyma

Previous studies found that in the LPS-induced endotoxemia mouse model, the BBB undergoes substantial disruption typically within 6 to 24 h post-LPS administration [48–50]. Our study firstly confirmed the impact of LPS on BBB integrity across a spectrum of low-to-sub-lethal doses, ranging from 10 mg/kg to 25 mg/kg body weight, in adult male C57BL/6J wild-type (WT) mice. Utilizing immunofluorescence (IF) staining to detect the extravasation of endogenous plasma immunoglobulin (IgG), we observed that LPS exposure led to extensive BBB leakage in a dose-dependent manner, and the 25 mg/kg dosage elicited the most pronounced and consistent effects at the 24 h following LPS injection, while the vascular area showed no obvious changes (Figure S1A-D). Consequently, the 25 mg/kg sub-lethal

dosage of LPS was selected for the establishment of the endotoxemia model and induction of persistent systemic inflammation in our study (Fig. 1A). At this dosage, the mortality rate was observed to be between 30% and 40% within the initial 24 h (Fig. 1B), with the surviving mice exhibiting markedly body weight loss (Fig. 1C), impaired motor function as evidenced by reduced spontaneous movement, increased jerky movements and abnormal gait, and piloerection, alongside partially closed eyes and a small amount of discharge from their eyes. Furthermore, the BBB in mice exposed to this LPS dosage demonstrated severe and extensive leakage to the exogenous tracer Evans Blue, together with the leakage of endogenous plasma IgG (Fig. 1D-E).

Considering that LPS causes tissue damages mainly by triggering systemic inflammatory responses, including elevation of massive proinflammatory factors in the circulation of both humans and mice [7, 51, 52], we further evaluated the effects of proinflammatory cytokines on BBB permeability using TNF-α. We observed that mice administered with high dosages of recombinant TNF-α (0.3 mg/kg and 0.4 mg/kg body weight, intravenous injection, once) all died within 6–8 h post-injection, whereas mice receiving low dosage of TNF-α (0.2 mg/kg body weight) were able to survive for more than 24 h and thus were subjected to further BBB analysis (Figure S2A-B). Importantly, we found that although the extent of BBB leakage was much less than that caused by LPS, TNF-α still led to significant BBB leakage, which was evidenced by extravasation of intravascular Evans Blue, plasma IgG and albumin into the brain tissue at 24 h after TNF-α injection (Figure S2C-E). This result also suggests that the BBB leakage caused by LPS may be the result of the additive or synergistic effects of multiple proinflammatory factors.

As expected, our subsequent evaluation of the inflammatory responses within the brain tissue revealed that the NF-κB pathway in brain endothelium was notably activated in response to LPS treatment, as evidenced by co-IF staining for blood vessel endothelium and the p65 subunit (Fig. 1F). In line with this, the expression level of VCAM1, a downstream gene of NF-κB pathway which facilitates leukocyte adhesion, was significantly elevated in brain ECs of LPS-treated mice (Fig. 1G). The presence of neuroinflammation in LPS-treated mice was further confirmed by an increase in the number and activation of $Iba1^+$ microglia (Fig. 1H). Notably, the $Iba1^+$ microglia cells became to attach and envelop blood vessels and exhibited an ameboid morphology in LPS-injected mice, in contrast to the saline control group in which microglia spread across the brain parenchyma (Fig. 1H). RT-qPCR analysis showed that the gene expression levels of proinflammatory cytokines and chemokines, including *Tnf*, *Il1b*, *Il6*, *Il17a* and *Ccl2*, were substantially upregulated in the brain tissue of LPS-treated mice when compared to the saline control, further underscoring the inflammatory response within the brain (Fig. 1I). In aggregate, these findings illustrate that LPS-induced endotoxemia leads to significant BBB disruption and triggers both vascular and neuroinflammatory responses.

LPS and proinflammatory cytokines suppresses brain endothelial Wnt/β-catenin signaling both in vivo and in vitro

In the context of endotoxemia, brain ECs are subjected to a barrage of circulating factors that may persistently compromise their integrity, with LPS and proinflammatory mediators being particularly detrimental. Given the pivotal role of the Wnt/β-catenin signaling pathway in the establishment and preservation of the BBB and that active β-catenin is specifically and abundantly expressed in the brain ECs, but is absent in pericytes/mural cells and minimally expressed in non-vascular cells (Figure S3A-B), we sought to investigate whether endothelial Wnt/β-catenin pathway is compromised by endotoxemia-induced systemic inflammation in both in vivo and in vitro models. IF staining in mice post-LPS injection revealed that the endothelial levels of active β-catenin (non-phosphorylated) and LEF1, a canonical Wnt signaling target gene which is instrumental in initiating β-catenin-dependent gene transcription [53], were both significantly reduced in brain ECs when compared to the saline control group (Fig. 2A-D, Figure S3B). To further elucidate this, we employed flow cytometry to acutely isolate pure brain ECs from mice treated with either LPS or saline and quantified the expression levels of Wnt/β-catenin signaling target genes using RT-qPCR. Our findings indicated that the mRNA levels of four key target genes (*Axin2*, *Apcdd1*, *Nkd1*, *Notum*) of brain endothelial Wnt/β-catenin signaling [54] were significantly diminished in brain ECs derived from LPS-treated mice, compared to those from saline-treated mice (Fig. 2E). This underscores the inhibitory effect of LPS on brain endothelial Wnt/β-catenin signaling.

Subsequently, we assessed whether LPS or proinflammatory factors directly modulate brain ECs to suppress Wnt/β-catenin signaling in vitro. Mouse brain microvascular ECs bEnd.3 were treated with recombinant Wnt3a protein (100 ng/ml) in the presence or absence of varying concentrations of LPS, TNF-α, IL-1β, IL-6, IL-17A, IFN-γ, and CCL2 for 24 h. We then determined the status of Wnt/β-catenin signaling by quantifying *Axin2* mRNA level and the TCF/LEF-dependent luciferase activity via the TOP-Flash assay. The data demonstrated that LPS, TNF-α, and IL-1β notably downregulated both *Axin2* expression (Fig. 2F-H) and Wnt/β-catenin signaling activity (Fig. 2I-K). Other proinflammatory factors, namely IL-6, IL-17A, IFN-γ, and CCL2, did not exert

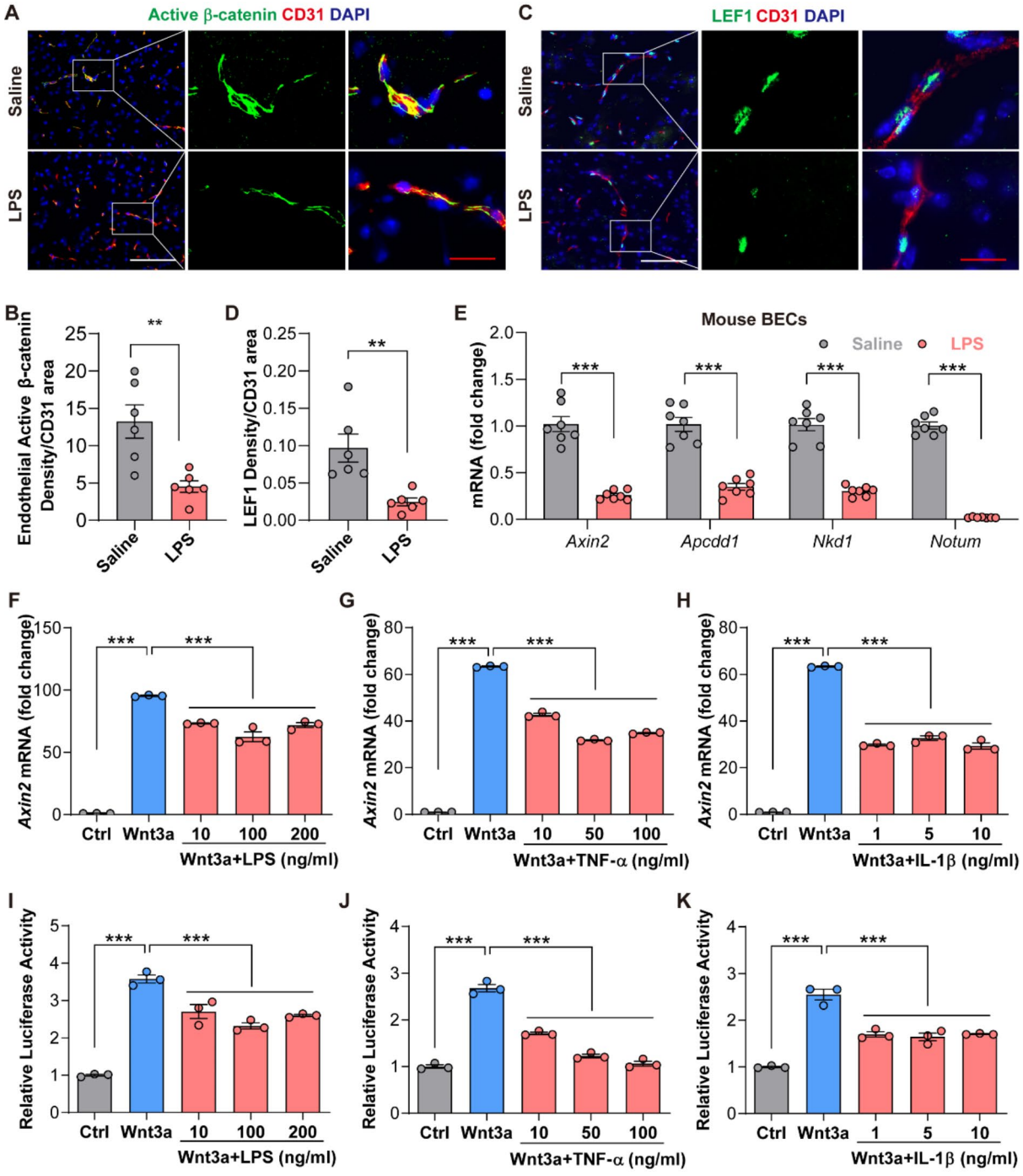

Fig. 2 LPS and proinflammatory cytokines suppress brain endothelial Wnt/β-catenin signaling. **A-B**, Co-immunofluorescence staining of active β-catenin (non-phosphorylated) and CD31 in the brain cortex tissue of mice treated with LPS or saline (**A**) and its quantifications (**B**). Active β-catenin signal in endothelial cells was selectively quantified. $n = 6$ mice per group. (**C-D**) Co-immunofluorescence staining of LEF1 and CD31 in the brain cortex tissue of mice treated with LPS or saline (**C**) and its quantifications (**D**). $n = 6$ mice per group. **E**, RT-qPCR analysis of the expression levels of Wnt/β-catenin signaling target genes *Axin2*, *Apcdd1*, *Nkd1*, and *Notum* in brain endothelial cells (ECs) isolated by flow cytometry from saline or LPS-treated mice (normalized to β-actin). $n = 7$ mice per group. **F-H**, RT-qPCR analysis of the expression levels of *Axin2* in mouse brain microvascular ECs (bEnd.3) treated with recombinant Wnt3a protein (100 ng/ml) or Wnt3a protein plus LPS (**F**), TNF-α (**G**), IL-1β (**H**) (normalized to β-actin). **I-K**, TOP-Flash assay in mouse brain microvascular ECs (bEnd.3) treated with recombinant Wnt3a protein (100 ng/ml) or Wnt3a protein plus LPS (**I**), TNF-α (**J**), IL-1β (**K**). $n = 3$ biological replicates per group. White scale bar: 100 μm. Red scale bar: 25 μm. Data are presented as mean ± SEM. $^{**}P < 0.01$, $^{***}P < 0.001$, Student's *t*-test for **B**, **D**, **E**, one-way ANOVA for **F-K**

significant influence on the Wnt/β-catenin signaling in bEnd.3 cells (Figure S4A-D). Taken together, our findings provide compelling evidence that LPS-induced endotoxemia suppresses the Wnt/β-catenin signaling pathway in brain ECs, an effect that is at least partially mediated through the exacerbation of systemic inflammation.

NF-κB p65 interacts with β-catenin and reduces β-catenin-dependent gene transcription in brain endothelium

Activation of the canonical Wnt signaling pathway, which is β-catenin-dependent, involves the liberation of cytosolic β-catenin from the Axin/APC/GSK3β/CK1α destruction complex. Once released, β-catenin becomes unphosphorylated, is stabilized, and subsequently translocates to the nucleus to facilitate the transcription of target genes [53, 55]. Our data showed that recombinant Wnt3a protein enhances the levels of both total and nuclear active β-catenin (non-phosphorylated) in bEnd.3 cells, while co-treatment with TNF-α and IL-1β significantly downregulated the levels of total and nuclear active β-catenin (Fig. 3A-C), indicating that TNF-α and IL-1β impeded the stabilization and translocation of β-catenin.

Since TNF-α and IL-1β primarily and potently activate the NF-κB pathway which showed intense crosstalk with Wnt/β-catenin signaling in other cell types [40, 56], we determined whether NF-κB pathway also interacts with Wnt/β-catenin signaling in brain ECs. As expected, TNF-α and IL-1β treatment led to the activation of NF-κB pathway shown by translocation of p65 from the cytoplasm to nucleus (Fig. 3D-E; Figure S5A-B) and upregulation of the vascular inflammation marker *Vcam1* expression (Figure S5C-D) in bEnd.3 cells. Importantly, we found that knockdown of the *p65* using siRNA or pharmacological inhibition of NF-κB pathway using BAY 11-7085, a small chemical molecule that inhibits phosphorylation of IκBa and NF-κB activation [57], could both effectively abolish the inhibitory effects of TNF-α and IL-1β treatment on Wnt3a-elicited activation of the Wnt/β-catenin signaling in bEnd.3 cells as evidenced by *Axin2* expression and TOP-Flash assay (Fig. 3F-G; Figure S5E-F). These results underscore the suppressive role of the NF-κB pathway on Wnt/β-catenin signaling in brain ECs.

Next, we further investigated the mechanism underlying the inhibitory effect of the NF-κB pathway on Wnt/β-catenin signaling in brain ECs. By recognizing that both p65 and β-catenin must translocate from the cytoplasm to the nucleus to fulfill their respective roles of transcriptional regulation, we hypothesized that a direct interaction between these two proteins might potentially impede the nuclear translocation of β-catenin. Due to the challenges associated with transfecting bEnd.3 cells with DNA plasmids, we utilized HEK 293T cells to test this hypothesis. The cells were simultaneously treated with recombinant Wnt3a protein and TNF-α to maximize the potential binding of p65 and β-catenin and assessed with bimolecular fluorescence complementation (BiFC) assay, which enable visualization of stable or dynamic protein-protein interactions in living cells [58]. The results indicate that upon activation by Wnt3a and TNF-α, p65 and β-catenin directly interacted with each other in both the cytoplasm and the nucleus (Fig. 3H). Co-immunoprecipitation (Co-IP) assays conducted in HEK 293T cells overexpressing HA-β-catenin and FLAG-p65 also demonstrated that Wnt3a and TNF-α co-treatment significantly enhanced the direct interaction between p65 and β-catenin (Figure S5G). Importantly, we observed that TNF-α treatment indeed reduced the nuclear translocation of β-catenin in the cells treated with Wnt3a compared to non-treated cells (Fig. 3H).

Lithium chloride (LiCl), known as an activator of the canonical Wnt signaling pathway in brain ECs [30], was shown to activate Wnt/β-catenin signaling activity in a dose-dependent manner and could partially restore Wnt3a-elicited β-catenin signaling activity even in the presence of TNF-α (Fig. 3I). This provides us a potential pharmacological approach to ameliorate endothelial Wnt/β-catenin signaling under inflammatory conditions.

In summary, our data suggest that pro-inflammatory factors downregulate Wnt/β-catenin signaling through activating NF-κB pathway and increasing the subsequent crosstalk between these two pathways.

Inhibition of NF-κB pathway in vivo upregulates endothelial Wnt/β-catenin signaling and attenuates BBB leakage induced by LPS

To further confirm the negative regulation of NF-κB pathway on endothelial Wnt/β-catenin signaling, we administered mice with the NF-κB inhibitor BAY 11-7085 which has been used in above cell experiments, at a dosage of 5 mg/kg body weight, 30 min post-LPS injection (Fig. 4A). We found that NF-κB inhibitor treatment could reduce the mortality rate (Fig. 4B) and significantly mitigate body weight loss (Fig. 4C) induced by LPS injection. Results also showed that the inhibitor led to a significant downregulation of NF-κB pathway in the brain endothelium, counteracting the heightened levels triggered by LPS (Fig. 4D). Concurrently, the expression of VCAM1, which is transcriptionally regulated by NF-κB signaling [59], was diminished by the inhibitor, whereas its expression was upregulated following LPS injection (Fig. 4E).

Given the observed reduction in NF-κB pathway and inflammation within the brain endothelium due to the inhibitor's intervention, we then investigated endothelial Wnt/β-catenin signaling and BBB integrity in endotoxemia mice. Notably, the endothelial expression of LEF1 (Fig. 4F) and non-phosphorylated β-catenin (Fig. 4G)

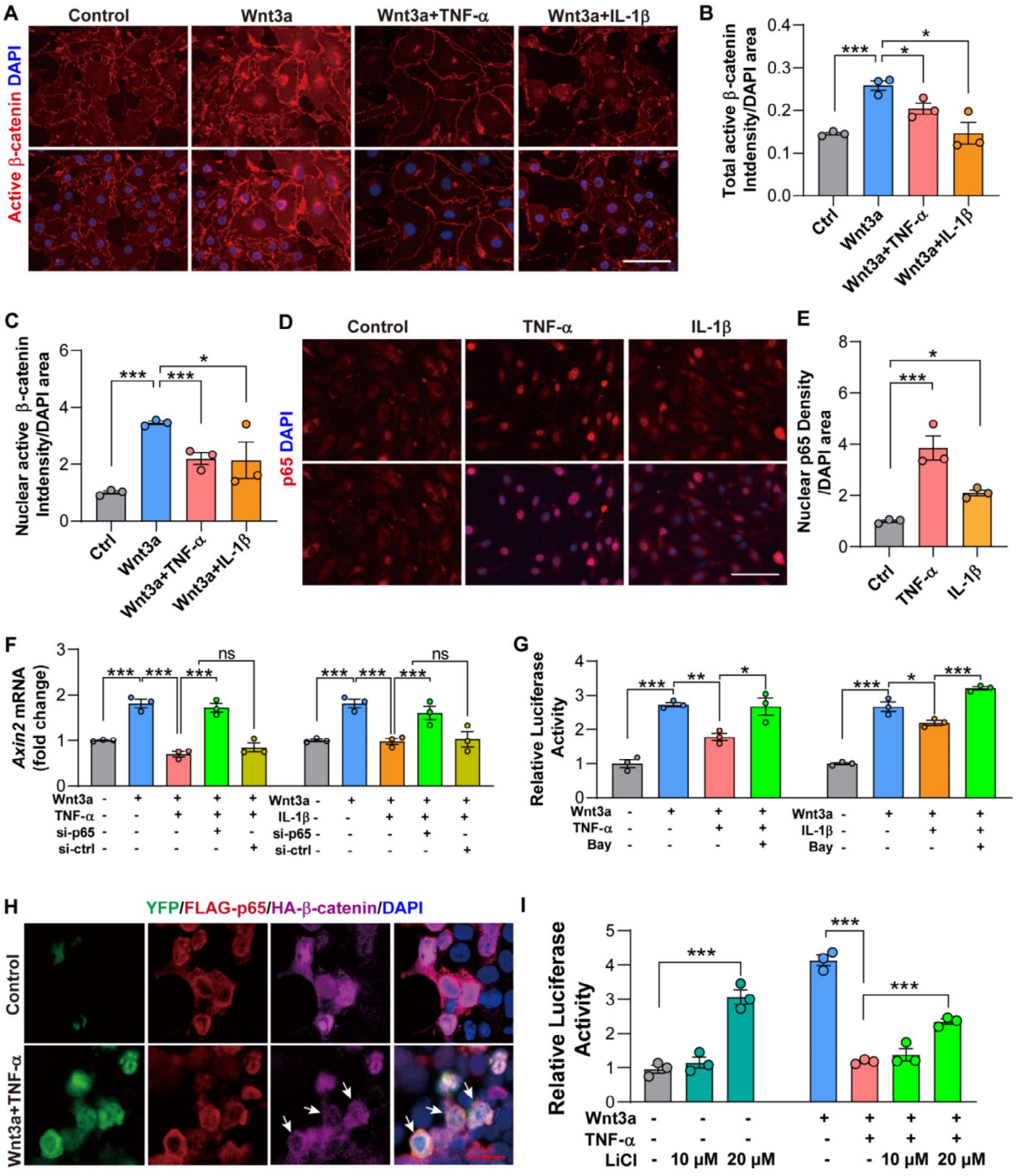

Fig. 3 NF-κB p65 interacts with β-catenin and reduces β-catenin-dependent gene transcription in brain endothelium. **A-C**, Immunofluorescence staining of active β-catenin (non-phosphorylated) in bEnd.3 cells treated with recombinant Wnt3a protein (100 ng/ml) only or Wnt3a protein plus TNF-α (100 ng/ml) or IL-1β (10 ng/ml) for 24 h and its quantifications presented as total signal intensity (**B**) and nuclear signal intensity (**C**). **D-E**, Immunofluorescence staining of NF-κB p65 in bEnd.3 cells treated with TNF-α or IL-1β and its quantifications presented as nuclear intensity. **F**, RT-qPCR analysis of the expression levels of Wnt target gene *Axin2* in bEnd.3 cells when NF-κB p65 was knocked down and the cells were treated with Wnt3a with or without TNF-α or IL-1β. **G**, TOP-Flash assay of bEnd.3 cells treated with NF-κB pathway inhibitor BAY 11-7085 (10 mM) and the cells were treated with Wnt3a with or without TNF-α or IL-1β. **H**, Bimolecular fluorescence complementation (BiFC) assay in HEK 293T cells treated with vehicle control or Wnt3a protein plus TNF-α. Arrows indicate cells with significantly reduced levels of β-catenin in the nucleus. **I**, TOP-Flash assay of bEnd.3 cells treated with Wnt3a protein, TNF-α, and LiCl. $n = 3$ replicates per group. White scale bar: 50 μm. Red scale bar: 20 μm. Data are presented as mean ± SEM. ns, no significance, $^{*}P < 0.05$, $^{**}P < 0.01$, $^{***}P < 0.001$, one-way ANOVA

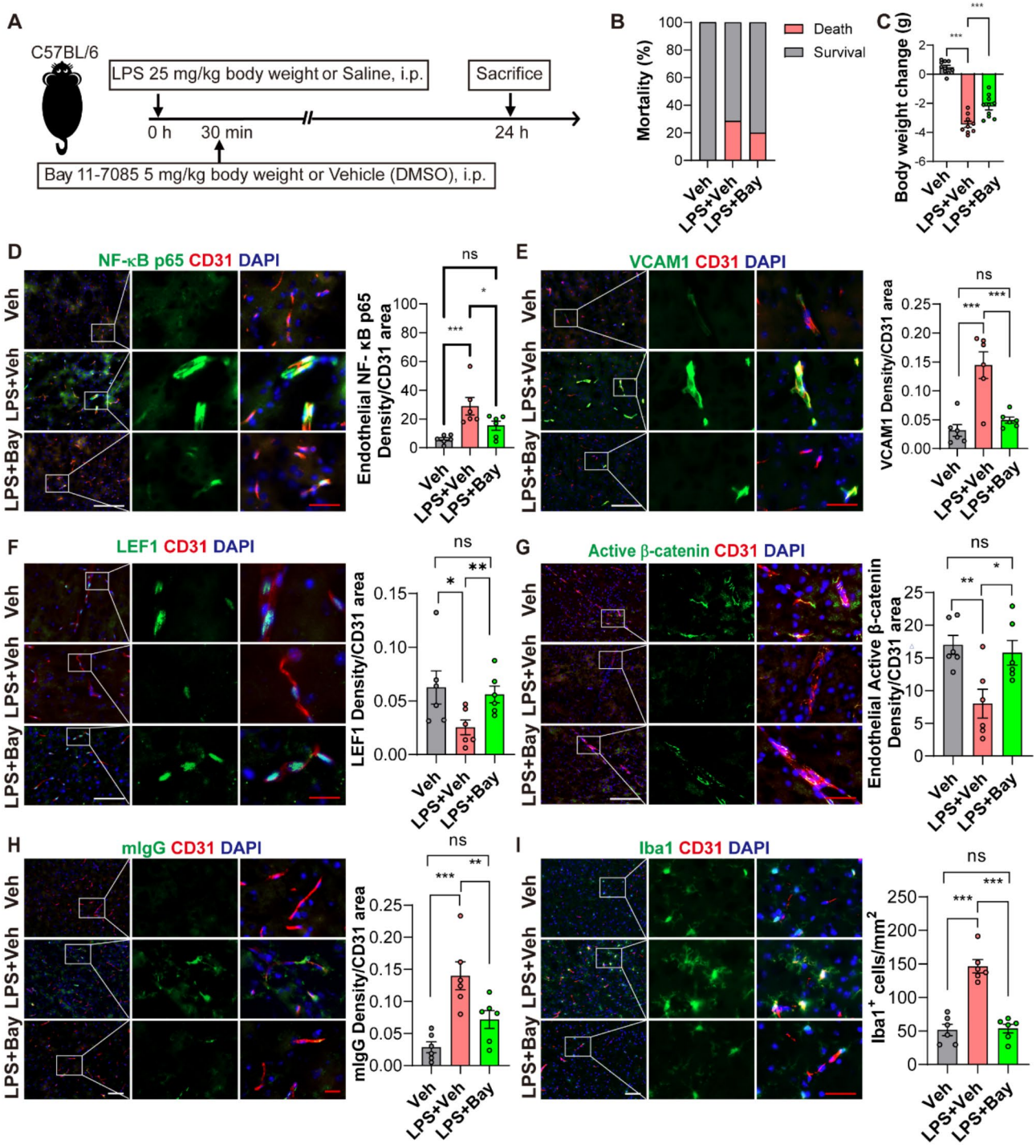

Fig. 4 Inhibition of NF-κB pathway in vivo restores brain endothelial Wnt/β-catenin signaling and attenuates LPS-induced BBB leakage and neuroinflammation. **A**, Schematic illustration of experimental design. The NF-κB pathway inhibitor BAY 11-7085 (5 mg/kg) or vehicle control (DMSO) was intraperitoneally (i.p.) injected to mice at 30 min after LPS or saline injection. **B**, Mortality rate of mice at 24 h following vehicle ($n = 10$ mice), LPS + vehicle ($n = 14$ mice), or LPS + BAY 11-7085 ($n = 15$ mice) treatment. **C**, Body weight change of the mice at 24 h after vehicle ($n = 10$ mice), LPS + vehicle ($n = 9$ mice), or LPS + BAY 11-7085 ($n = 10$ mice) treatment. **D**, Co-immunofluorescence staining of NF-κB p65 and CD31 in the brain cortex and its quantifications. NF-κB p65 signal in endothelial cells was selectively quantified. **E**, Co-immunofluorescence staining of VCAM1 and CD31 in the brain cortex and its quantifications. **F**, Co-immunofluorescence staining of LEF1 and CD31 in the brain cortex and its quantifications. **G**, Co-immunofluorescence staining of active β-catenin (non-phosphorylated) and CD31 in the brain cortex and its quantifications. Active β-catenin signal in endothelial cells was selectively quantified. **H**, Co-immunofluorescence staining of mouse plasma IgG and CD31 in the brain cortex and its quantifications. **I**, Co-immunofluorescence staining of Iba1$^+$ microglia and CD31 in the brain cortex and its quantifications. $n = 6$ mice per group for **D-I**. White scale bar: 100 μm. Red scale bar: 25 μm. Data are presented as mean ± SEM. $^*P < 0.05$, $^{**}P < 0.01$, $^{***}P < 0.001$, one-way ANOVA for **C-I**

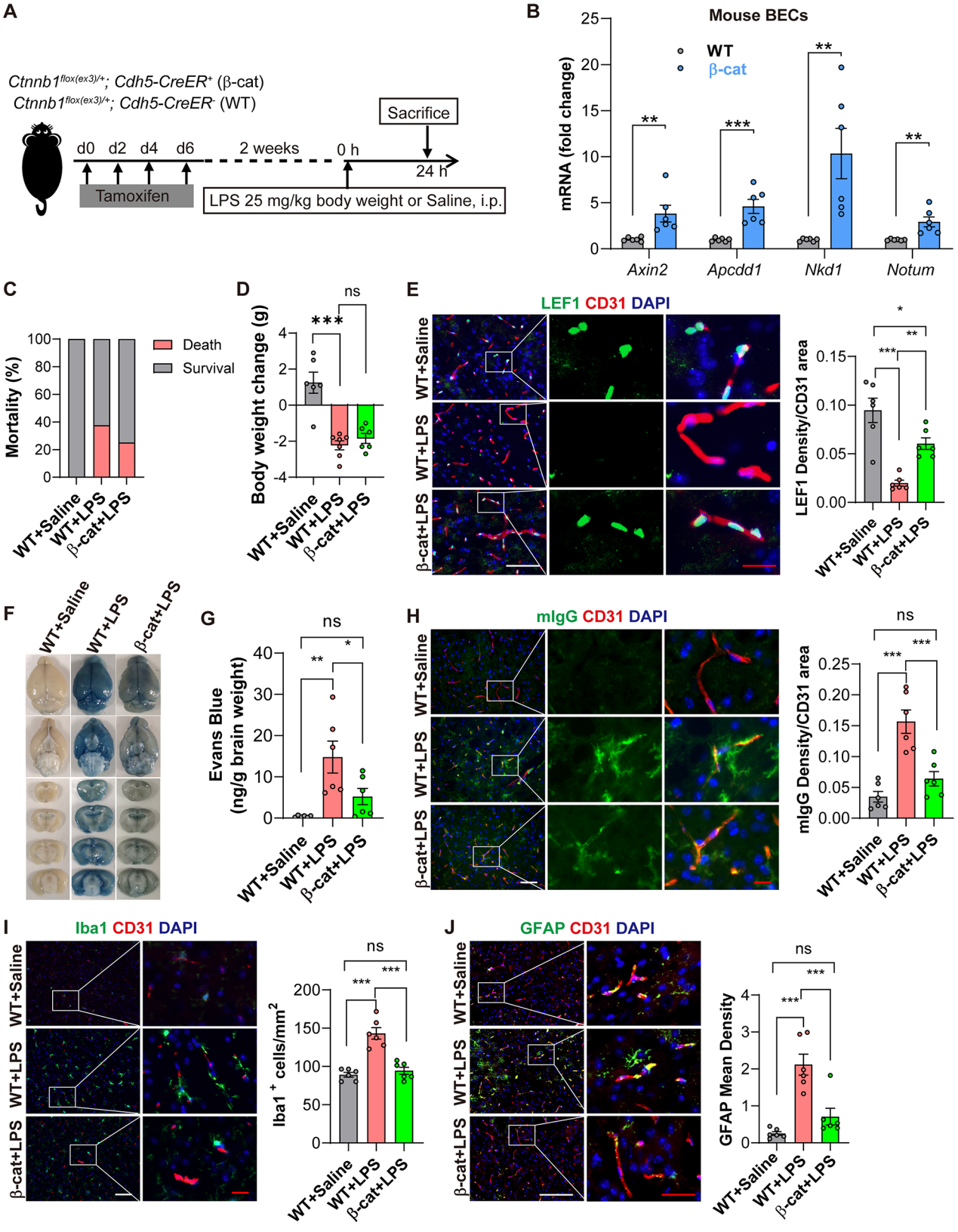

Fig. 5 (See legend on next page.)

(See figure on previous page.)

Fig. 5 Genetic activation of endothelial Wnt/β-catenin signaling in vivo mitigates LPS-induced BBB leakage and neuroinflammation. **A**, Schematic illustration of experimental design for the induction of β-catenin (encoded by *Ctnnb1*) constitutive activation in mice with LPS-induced endotoxemia. **B**, RT-qPCR analysis of the expression levels of Wnt/β-catenin signaling target genes *Axin2*, *Apcdd1*, *Nkd1*, and *Notum* in brain endothelial cells (ECs) isolated by flow cytometry from WT or β-cat mice (normalized to β-actin). **C**, Mortality rate of WT and β-cat mice at 24 h following Saline or LPS treatment. WT + Saline ($n = 10$ mice), WT + LPS ($n = 16$ mice), β-cat + LPS ($n = 8$ mice). **D**, Body weight change of the mice at 24 h after Saline or LPS injection. WT + Saline ($n = 6$ mice), WT + LPS ($n = 7$ mice), β-cat + LPS ($n = 6$ mice). **E**, Co-immunofluorescence staining of LEF1 and CD31 in the brain cortex and its qualifications. **F-G**, Representative brain images showing Evans Blue leakage and its qualifications presented as nanogram dye per gram brain weight (ng/g). **H**, Co-immunofluorescence staining of mouse plasma IgG and CD31 in the brain cortex and its qualifications. **I**, Co-immunofluorescence staining of Iba1 and CD31 in the brain cortex and its qualification. **J**, Co-immunofluorescence staining of GFAP and CD31 in the brain and its qualification. $n = 6$ mice per group for **E-J**. White scale bar: 100 μm. Red scale bar: 25 μm. Data are presented as mean ± SEM. $^{*}P < 0.05$, $^{**}P < 0.01$, $^{***}P < 0.001$. Student's *t*-test for **B**, one-way ANOVA for **D-J**

exhibited an upregulation upon the treatment with BAY 11-7085 subsequent to LPS injection. This suggested that inhibition of NF-κB pathway can prevent the decline of Wnt/β-catenin signaling that is typically induced by LPS. Consistently, the BBB leakage, as evidenced by the mouse plasma IgG extravasation into the brain tissue, was significantly reduced by the inhibitor when compared to the LPS-only group (Fig. 4H).

Moreover, the number of $Iba1^{+}$ microglia, indicative of microglia activation, within the brains of mice co-administrated with LPS plus BAY 11-7085 was markedly lower than that in those administrated with LPS alone (Fig. 4I). These results provide in vivo evidences that NF-κB pathway inhibits endothelial Wnt/β-catenin signaling and contributes to BBB disruption in mice with endotoxemia.

Genetic activation of endothelial Wnt/β-catenin signaling attenuates the BBB leakage and neuroinflammation caused by LPS

In this part, we employed a β-catenin exon3 flox allele to investigate the role of endothelial Wnt/β-catenin signaling in BBB disruption induced by endotoxemia. Exon3 deletion results in deletion of phosphorylation sites of β-catenin protein, making it resistant to ubiquitination-dependent degradation while preserving its transcription activation function, and thus constitutive activation of β-catenin-dependent signaling [45]. Firstly, we generated the inducible β-catenin endothelium-conditional activation mice (*Ctnnb1*$^{\text{flox (ex3) /+}}$; *Cdh5*-CreER^{+}, termed β-cat) and their WT littermates (*Ctnnb1*$^{\text{flox (ex3) /+}}$; *Cdh5*-CreER^{-}, termed WT). We aimed to determine whether the activation of endothelial Wnt/β-catenin signaling could offer protection to BBB against endotoxemia. β-cat mice and WT littermates were administrated with tamoxifen two weeks before treatment with LPS to induce endotoxemia as described above (Fig. 5A). The brain ECs were sorted using flow cytometry and the mRNA levels of several Wnt/β-catenin signaling targets, including *Axin2*, *Apcdd1*, *Nkd1*, and *Notum*, were found to be upregulated (Fig. 5B), suggesting that brain endothelial Wnt/β-catenin signaling was activated in β-cat mice.

Upon the establishment of the endotoxemia model in these mice, the β-cat mice showed reduced mortality rate and a trend of less body weight loss compared to WT mice after LPS injection (Fig. 5C-D). For the endothelial Wnt/β-catenin pathway, we noted a significant increase in the expression of LEF1 in brain ECs of β-cat mice compared to WT littermates after LPS challenge, although it did not fully return to baseline levels (Fig. 5E), indicating the amelioration of endothelial Wnt/β-catenin signaling in β-cat mice. The reduced extravasation of Evans Blue and mouse plasma IgG into the brains of β-cat mice suggested a mitigation of LPS-induced BBB leakage, which was likely attributable to the activation of Wnt/β-catenin signaling in brain ECs (Fig. 5F-H). Furthermore, the activation of microglia ($Iba1^{+}$ cells) and astrocyte ($GFAP^{+}$ cells) in the brains of β-cat mice were both significantly diminished, compared to LPS-administrated WT mice (Fig. 5I-J). These results suggest that activation of Wnt/β-catenin signaling specifically in brain ECs can ameliorate BBB disruption and neuroinflammation in endotoxemia mice.

Downregulation of Wnt/β-catenin signaling by conditional ablation of endothelial Gpr124 aggravates the BBB leakage caused by LPS

Our previous study has demonstrated that endothelial Gpr124, the Wnt7a/7b-specific co-receptor [60–62], is of little account in BBB integrity of adult mice under homeostatic conditions, while its deletion significantly downregulates Wnt signaling and exacerbates BBB disruption under pathological conditions [27]. Here we developed a milder endotoxemia model dosed with 18 mg/kg body weight LPS in mice without or with Gpr124 endothelial conditional knockout (*Gpr124*$^{\text{flox/flox}}$; *Cdh5*-CreER^{+}, termed ECKO; *Gpr124*$^{\text{flox/flox}}$; *Cdh5*-CreER^{-}, termed WT, respectively) (Figure S6A). The results revealed a more pronounced BBB leakage in Gpr124 ECKO mice compared to their WT littermates, evidence by an increased extravasation of mouse plasma IgG and albumin into the brain of Gpr124 ECKO mice post-LPS injection (Figure S6B-C). These data indicate

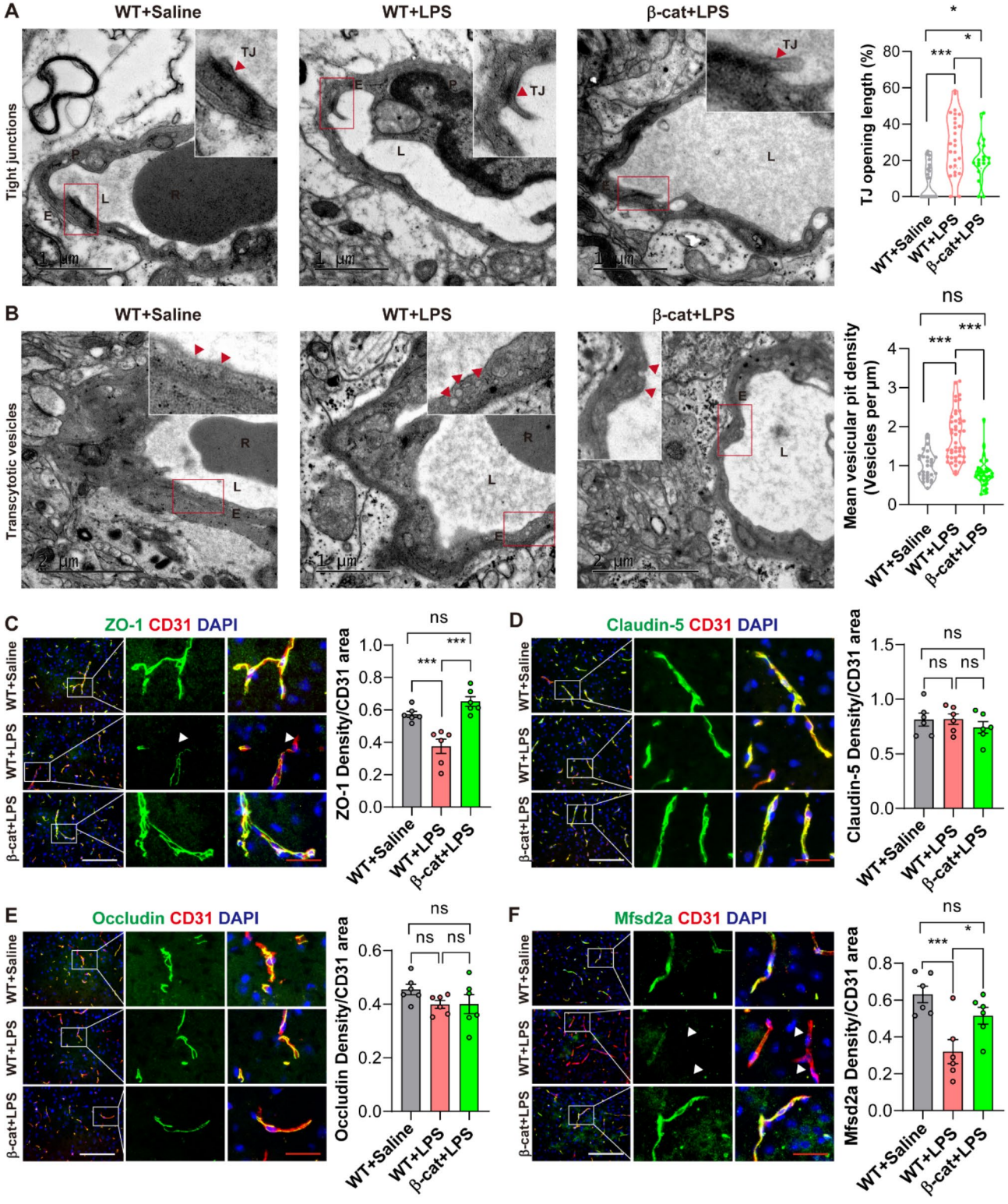

Fig. 6 (See legend on next page.)

(See figure on previous page.)

Fig. 6 Genetic activation of endothelial Wnt/β-catenin signaling in vivo improves tight junctions and reduces transcytosis in mice treated with LPS. **A**, Representative TEM images from mouse brain cortex tissue showing tight junctions opening induced by LPS and its quantifications presented as percentage of the opening length of the whole tight junction length. $n = 3$ to 4 mice per group, and each data point represents one tight junction structure. **B**, Representative TEM images from mouse brain cortex tissue showing endothelial vesicles and its quantifications presented as mean vesicular pit density (vesicles per um endothelial profile). $n = 3$ to 4 mice per group, and each data point represents one capillary. P, Pericyte; E, endothelial cell; L, lumen; R, red blood cells; TJ, tight junctions. **C-E**, Co-immunofluorescence staining of tight junction proteins ZO-1 **(C)**, Claudin-5 **(D)**, Occludin **(E)** and CD31 and quantifications in the mouse brain cortex tissue. White arrows indicate blood vessels with loss of ZO-1 expression. **F**, Co-immunofluorescence staining of the transcytosis suppressor Mfsd2a and CD31 and its quantifications in the mouse brain cortex tissue. White arrows indicate blood vessels with loss of Mfsd2a expression. $n = 6$ mice per group for **C-F**. White scale bar: 100 μm. Red scale bar: 25 μm. Data are presented as mean ± SEM. ns, no significance, $^{*}P < 0.05$, $^{***}P < 0.001$, one-way ANOVA

that downregulation of Wnt/β-catenin signaling specifically in brain ECs aggravates BBB breakdown induced by endotoxemia.

Endothelial Wnt/β-catenin signaling regulates LPS-caused BBB leakage through inhibition of both paracellular and transcellular passage pathways

We previously observed the downregulation of endothelial Wnt/β-catenin signaling causes BBB disruption by enhancing both paracellular and transcellular permeability [63]. Therefore, we investigated tight junctions (TJs) and transcytosis in endotoxemia mice using transmission electron microscopy (TEM). Results showed that LPS significantly disrupted tight junctions in ultrastructure of BBB in WT mice, and this disruption was effectively counteracted by genetic activation of β-catenin (Fig. 6A). Transcytosis, another distinguished function of BBB, is usually evaluated by counting the number of vesicles in brain capillary ECs [23]. A noticeable increase in vesicle counts was observed in the brain endothelium of WT mice treated with LPS compared to untreated WT mice, whereas this increase was nearly abolished in β-cat mice treated with LPS (Fig. 6B), indicating a substantial suppression of endothelial transcytosis by β-catenin activation. At the molecular level, IF staining showed that the expression level of tight junction protein ZO-1 was significantly decreased by LPS treatment in WT mice and fully restored in β-cat mice treated with LPS, and leakage of plasma IgG can be observed in vessels with loss of ZO-1 expression in WT mice treated with LPS group (Fig. 6C, Figure S3C-E). In contrast, the other two TJs proteins, Claudin-5 and Occludin, did not exhibit reductions by LPS in WT mice (Fig. 6D-E, Figure S3E). The staining result for Mfsd2a, a potent suppressor of transcytosis, showed that Mfsd2a was significantly reduced by LPS treatment compared to saline treatment in WT mice, in line with a previous report [64]. Importantly, β-catenin activation significantly increased the expression of Mfsd2a in β-cat mice treated with LPS to levels comparable to those seen in WT mice treated with saline, paralleling the TEM findings about endothelial vesicles (Fig. 6F).

Pharmacological activation of endothelial Wnt/β-catenin signaling attenuates the BBB leakage and neuroinflammation caused by LPS

Finally, we selected lithium chloride (LiCl) as an alternative method to activate Wnt/β-catenin signaling and investigated its protective effects on LPS-induced BBB leakage. Under normal conditions, LiCl treatment at the dosage of 3 mmol/kg did not cause mouse death or obvious body weight loss, but led to a significant upregulation of Wnt/β-catenin signaling in the brain endothelium (Figure S7A-D). In addition, LiCl treatment at this dosage did not affect neuroinflammation (no changes in microglia or astrocytes) or BBB integrity (Figure S7E-J). Therefore, we further evaluated the therapeutic potential of 3 mmol/kg LiCl treatment in mice injected with LPS (Fig. 7A). We observed that the mortality rate of mice was reduced by LiCl treatment while body weight loss was inclined to be less severe (Fig. 7B, C). Consistent with our in vitro findings (Fig. 3I), LiCl administration led to a significant upregulation of Wnt/β-catenin signaling in the brain endothelium of LPS-treated mice (Fig. 7D-E). BBB leakage is effectively attenuated by LiCl treatment as evidenced by the staining for mouse plasma IgG (Fig. 7F) and Evans Blue leakage into the brain parenchyma (Fig. 7G-H). Moreover, LiCl treatment reduced the neuroinflammation triggered by LPS, as assessed by the activation of microglia ($Iba1^{+}$ cells) (Fig. 7I) and astrocytes ($GFAP^{+}$ cells) (Fig. 7J), and the expression levels of proinflammatory cytokines and chemokines, including *Tnf*, *Il1b*, *Il6*, and *Ccl2*(Fig. 7K). Taken together, as a small molecular drug that has been used in clinic for decades, LiCl treatment holds promise to ameliorate BBB disruption caused by endotoxemia.

Discussion

Systemic inflammation during sepsis often causes acute neurological dysfunction, and many patients continue to experience cognitive impairment long after recovering from sepsis. The impairment of BBB integrity promotes the development of SAE [50, 65], whereas the mechanism of sepsis-associated BBB breakdown is still unclear at the moment. In the current study, we found that compromised endothelial Wnt/β-catenin signaling was responsible for the acute BBB disruption in endotoxemia.

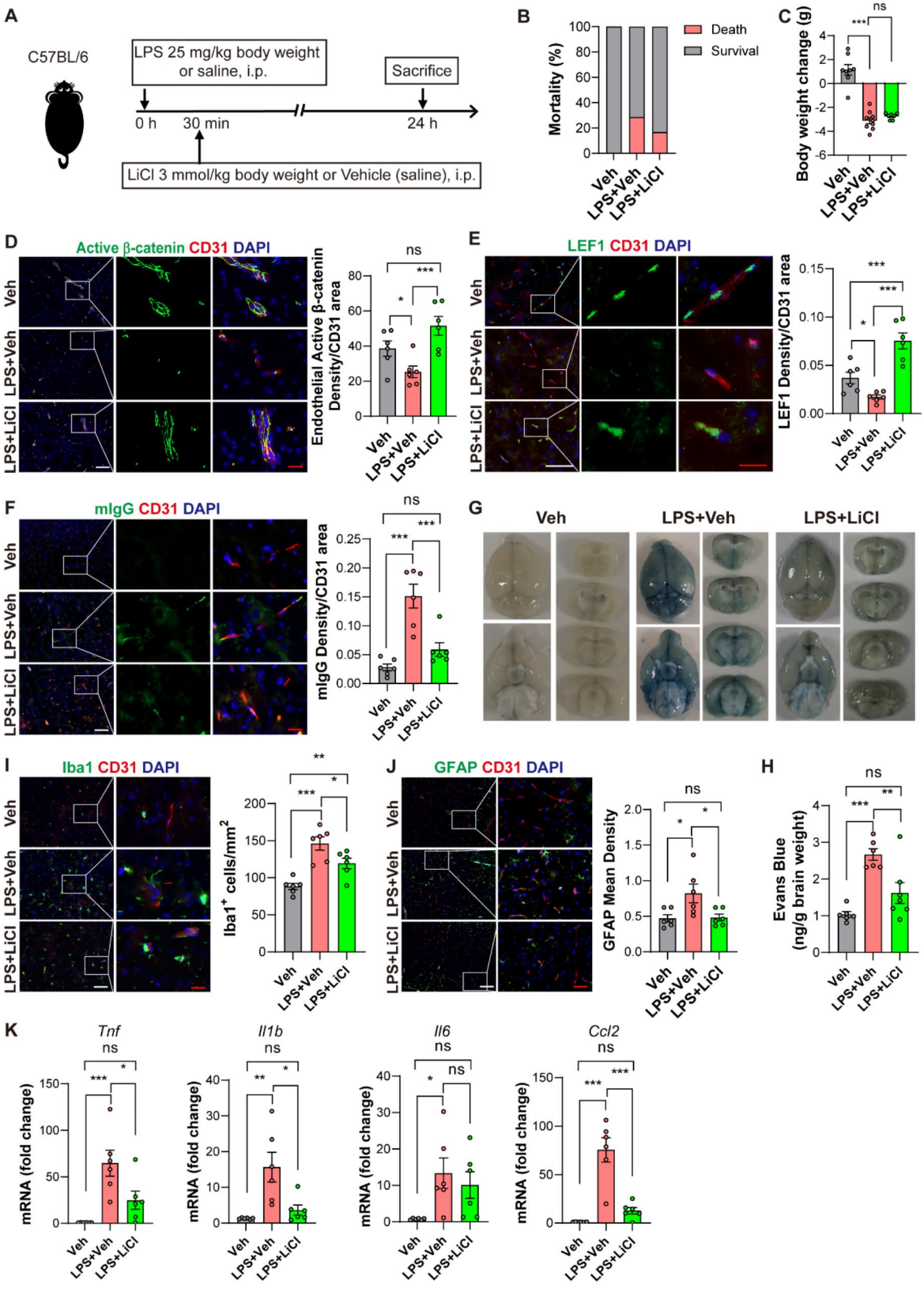

Fig. 7 (See legend on next page.)

(See figure on previous page.)

Fig. 7 Lithium upregulates brain endothelial Wnt/β-catenin signaling and attenuates LPS-induced BBB leakage and neuroinflammation. **A**, Schematic illustration of experimental design. The Wnt/β-catenin signaling pathway agonist Lithium (3 mmol/kg) or vehicle control (saline) was intraperitoneally (i.p.) injected to mice at 30 min after LPS or saline injection. **B**, Mortality rate of mice at 24 h following vehicle ($n=12$ mice), LPS + vehicle ($n=14$ mice), or LPS + LiCl ($n=12$ mice) treatment. **C**, Body weight change of mice at 24 h following vehicle ($n=8$ mice), LPS + vehicle ($n=9$ mice), or LPS + LiCl ($n=7$ mice) treatment. **D**, Co-immunofluorescence staining of active β-catenin (non-phosphorylated) and CD31 in the brain cortex and its quantifications. Active β-catenin signal in endothelial cells was selectively quantified. **E**, Co-immunofluorescence staining of LEF1 and CD31 in the brain cortex and its quantifications. **F**, Co-immunofluorescence staining of mouse plasma IgG and CD31 in the brain cortex and its quantifications. **G-H**, Representative brain images showing Evans Blue leakage and its quantifications presented as nanogram dye per gram brain weight (ng/g). **I**, Co-immunofluorescence staining of $Iba1^+$ microglia and CD31 in the brain cortex and its quantifications. **J**, Co-immunofluorescence staining of GFAP and CD31 in the brain cortex and its quantifications. **K**, RT-qPCR analysis of the expression levels of proinflammatory factors *Tnf*, *Il1b*, *Il6*, and *Ccl2* in the brain cortex tissue (normalized to β-actin). $n=6$ mice per group for **D-K**. White scale bar: 100 μm. Red scale bar: 25 μm. Data are presented as mean ± SEM. ns, no significance, $^*P<0.05$, $^{**}P<0.01$, $^{***}P<0.001$, one-way ANOVA

Endotoxin (LPS) itself and the proinflammatory cytokines induced by endotoxin led to brain endothelial NF-κB p65 activation, which further suppressed Wnt/β-catenin signaling. Our in vivo data indicated that improving the activity of Wnt/β-catenin signaling in brain ECs, either directly by genetic and pharmacological approaches or indirectly by inhibiting NF-κB p65 pathway, could ameliorate BBB disruption and neuroinflammation in endotoxemia.

β-catenin-dependent canonical Wnt signaling is specific to CNS in blood vascular system [66]. Its constant activation is required for the maintenance of BBB in adults [21, 25, 67]. Conversely, downregulation of Wnt/β-catenin signaling usually results in BBB dysfunction. For example, transient inhibition of Unc5B, an up upstream molecule of the Wnt/β-catenin signaling, leads to rapid BBB leakage within an hour [68]. Furthermore, our previous studies showed that weakened endothelial Wnt/β-catenin signaling promotes stroke-induced acute BBB breakdown [27, 28, 30]. In the present study, LPS induced BBB leakage and a decline in endothelial Wnt/β-catenin signaling simultaneously. Additionally, the BBB leakage could be rescued by alteration of endothelial Wnt/β-catenin signaling through genetic (endothelial-specific β-catenin activation) and pharmacological (LiCl) approaches. Meanwhile, the upregulated Wnt/β-catenin signaling effectively alleviated neuroinflammation in endotoxemia mice. These results demonstrate that the decline of endothelial Wnt/β-catenin signaling mediates BBB disruption in endotoxemia. Moreover, our work indicates that endothelial Wnt/β-catenin signaling could be a potential therapeutic target for BBB protection in sepsis, for instance, through the use of Lithium. Lithium, an agonist of Wnt/β-catenin signaling used in the present study, is a clinical drug extensively used for treating bipolar mood disorders. Our previous work has demonstrated its BBB-protective effects in mouse stroke models [69, 70].

We previously identified endothelial Wnt/β-catenin signaling maintains the integrity of the adult BBB by inhibiting both the paracellular and transcellular permeability with β-catenin ECKO mice [63]. Correspondingly, our data indicate that endotoxin-induced decline of endothelial Wnt/β-catenin signaling mediated BBB leakage likely through both paracellular and transcytosis pathways. Compared to TJ associated paracellular pathway, studies on SAE paid few attentions on transcytosis-mediated BBB leakage. Until last year, Lei et al. reported that *Porphyromonas gingivalis* bacteremia increases Mfsd2a/Cav-1 mediated transcytosis in brain ECs [71]. To our knowledge, this is the first and only report on transcytosis-mediated BBB disruption in sepsis. However, transcytosis has been established as an early event related to BBB breakdown following pathological insults such as ischemic stroke [72]. We also observed an endotoxin-induced downregulation of Mfsd2a expression in brain ECs. Mfsd2a inhibits Cav-1-positive vesicle formation by regulating lipid environment of brain ECs, which is essential for BBB homeostasis [73]. Furthermore, we have shown that Mfsd2a expression is directly and positively regulated by Wnt/β-catenin signaling in brain ECs [25]. Here we observed that Mfsd2a expression was restored by genetically activating endothelial Wnt/β-catenin signaling, which completes the link between Wnt signaling and transcytosis-mediated BBB disruption in SAE development.

Another question is how endotoxin suppresses constitutive Wnt/β-catenin signaling in brain ECs. Firstly, LPS can be recognized by receptors located on the cell membrane and inside cells, such as Toll-like receptors (TLRs), CD14 and caspases, which trigger inflammatory activation of cells [74–77]. Secondly, LPS leads to a robust systemic inflammation, accompanied by increased circulating levels of proinflammatory cytokines, such as TNF-α and IL-1β, upon LPS challenge in both humans and mice [51, 52]. A previous study reported that the intravenous injection of proinflammatory cytokines, such as TNF-α and IL-1β, were sufficient to induce brain endothelial NF-κB pathway activation and VCAM1 expression, which further led to microglia activation, implying BBB disruption caused by circulating proinflammatory factors [78]. Our data indicate that both LPS and TNF-α could cause BBB leakage in mice and downregulated Wnt/β-catenin signaling in cultural brain ECs.

Given this information, we further identified an inhibitory effect of their common downstream NF-κB p65 on endothelial Wnt/β-catenin signaling. Although several reports have described the crosstalk between these two signaling pathways, what is particularly interesting is that the two signaling pathways can regulate each other in opposing directions depending on the tissue or situation. Take the regulation of NF-κB pathway on Wnt/β-catenin signaling as an example, activation of NF-κB pathway downregulates Wnt/β-catenin signaling in lung and bone, while it upregulates Wnt/β-catenin signaling in periapical tissue [79–81]. These findings suggest that the NF-κB pathway may influence Wnt/β-catenin signaling in a tissue- or cell-specific manner. Our in vitro and in vivo experiments collectively demonstrated that the NF-κB signaling activated by inflammatory stimulus suppresses Wnt/β-catenin pathway in brain ECs. In line with our results, a recent study reported that IL-1β inhibits endothelial Wnt/β-catenin signaling, leading to disruption of BBB development in zebrafish [82]. Deng et al. reported that β-catenin is able to form complex with NF-κB proteins [83]. Consistently, we visualized the interaction between NF-κB p65 and β-catenin using BiFC experiment. Taken together, our data suggest NF-κB p65 may inhibit β-catenin activity through direct physical contact with β-catenin.

Mechanistically, the present study focused on the interaction of NF-κB p65 and Wnt/β-catenin signaling in brain ECs, aiming to understand the underlying mechanisms that lead to the suppression of endothelial Wnt/β-catenin signaling in response to endotoxin exposure. The high level accumulation of non-phosphorylated β-catenin$^{Ser33/37/Thr41}$ (active form) protein in cytoplasm is essential for nucleus translocation of β-catenin to regulate transcription [84]. We observed a decrease in active β-catenin protein level in brain ECs both in vivo and in vitro following LPS or inflammatory cytokines stimulation. This suggests that the assembly of NF-κB/β-catenin complex may promote the degradation of β-catenin protein, thereby inhibiting Wnt/β-catenin signaling in brain ECs. GSK-3β or PKC mediates the ubiquitination and degradation of β-catenin protein by inducing β-catenin protein phosphorylation at Ser33/37 and Thr41 [85]. Accordingly, we show that the degradation-resistant β-catenin mutant protein lacking the GSK-3β-phosphorylation sites in the exon3 was able to rescue LPS-induced decline of endothelial Wnt/β-catenin signaling and BBB disruption in vivo. In addition, LiCl, an inhibitor of GSK-3β, is able to prevent GSK-3β-mediated β-catenin phosphorylation [86]. The rescue effects on Wnt/β-catenin signaling in vitro and in vivo in brain ECs by LiCl in the present study further support our speculation.

Additionally, our findings build a bridge between inflammation signal transduction (NF-κB) with constitutive signaling (endothelial Wnt/β-catenin signaling) in adult BBB dysfunction. Considering the widespread existence of BBB disruption in many systemic inflammation-associated situations [12], is the crosstalk between endothelial NF-κB and Wnt/β-catenin signaling a common mechanism involved in BBB disruption induced by systemic inflammation? In recent years, the pandemic of coronavirus disease 2019 (COVID-19) caused by severe acute respiratory syndrome coronavirus 2 (SARS-CoV-2) is the most severe global public health emergency, which has led to millions of deaths. Cytokine storm is a common clinical manifestation in patients with severe COVID-19, which is a hyperinflammatory medical condition induced by uncontrolled release of proinflammatory cytokines [87]. Meanwhile, BBB damage was found during COVID-19 [88]. Interestingly, recent studies found that SARS-CoV-2 infection causes BBB dysfunction via inhibiting Wnt/β-catenin signaling in brain ECs, and engineered Wnt7a ligands rescue BBB and cognitive deficits in a COVID-19 mouse model [89, 90]. In addition to various types of sepsis, other conditions such as chimeric antigen receptor-modified T (CAR-T) cell therapy, which is designed for tumor treatment, often leads to severe systemic inflammation and neurotoxicity [12]. The occurrence of neurotoxicity and BBB disruption in patients treated with CAR-T cell therapy correlates with elevated levels of serum cytokines [91]. The disruption of BBB not only leads to acute neurological disorders, but also increases the susceptibility to CNS diseases, such as Alzheimer's disease (AD), Parkinson's disease (PD), multiple sclerosis (MS), and stroke [92]. Therefore, further study on the mechanisms of the disruption of the BBB under various acute or chronic pathological conditions involving systemic inflammation, especially the role of endothelial Wnt/β-catenin signaling, is of great significance.

In addition to activating the NF-κB-Wnt/β-catenin signaling axis, LPS may also induce BBB disruption through alternative pathways. A recent study revealed that acute LPS treatment led to BBB breakdown in mice via GSDMD-mediated endothelial pyroptosis [93]. The pore-forming protein GSDMD was activated by the cytosolic LPS sensor caspase-11, not by TLR4-induced cytokines. Notably, that study administered a lethal dose of LPS (54 mg/kg) to mice and sacrificed them 8 h later, whereas we used a sub-lethal dosage of 25 mg/kg to induce systemic inflammation, a condition under which most mice could survive for over 24 h. It is plausible that different pathways may be involved in BBB disruption in response to varying degrees of systemic inflammation. Further research is warranted to validate this hypothesis.

Conclusions

Our research reveals a mechanism underlying endotoxemia-induced BBB disruption. Endotoxemia-associated systemic inflammation can inhibit endothelial Wnt/β-catenin signaling through activating NF-κB pathway, which leads to acute BBB disruption. The breakdown of BBB caused by endotoxemia includes damage of TJs and increase of transcytosis in brain ECs. We also demonstrate that BBB function is enhanced by inhibiting endothelial NF-κB pathway or upregulating endothelial Wnt/β-catenin signaling in endotoxemia. Our findings suggest that these two endothelial signaling pathways are promising therapeutic targets of endotoxemia-induced BBB disruption.

Abbreviations

AD	Alzheimer's disease
Axin2	Axis inhibition protein 2
BBB	Blood-brain barrier
CCL2	C-C Motif Chemokine Ligand 2
CNS	Central nervous system
ECs	Endothelial cells
GFAP	Glial fibrillary acidic protein
Iba1	Ionized calcium binding adaptor molecule 1
IFN-γ	Interferon gamma
IgG	Immunoglobulin
IL-1β	Interleukin-1 beta
IL-6	Interleukin-6
IL-17A	Interleukin-17A
LEF1	Lymphoid enhancer-binding factor 1
LiCl	Lithium chloride
LPS	Lipopolysaccharide
Mfsd2a	Major facilitator superfamily domain-containing protein 2
MS	Multiple sclerosis
NF-κB	Nuclear factor-kappa B
PDGFRβ	Platelet-derived growth factor receptor beta
SAE	Sepsis-associated encephalopathy
TCF/LEF	T-cell factor/lymphoid enhancer factor
TEM	Transmission electron microscopy
TNF-α	Tumor necrosis factor alpha
VCAM1	Vascular cell adhesion protein 1
ZO-1	Zonula occludens-1

Supplementary Information

The online version contains supplementary material available at https://doi.org/10.1186/s12974-024-03261-x.

Supplementary Material 1

Supplementary Material 2

Acknowledgements

The authors are grateful to Dr. Haitao Wu from Beijing Institute of Basic Medical Sciences for generously providing the *Ctnnb1* (β-catenin) exon3 flox mice.

Author contributions

X.H., P.W., C.F., M.Y., S.Y., and L.Q. performed the research; X.H. and P.W. analyzed the experimental data and wrote the manuscript; J.C. supervised the laboratory experiments and wrote the manuscript; and all other authors reviewed and commented the manuscript.

Funding

This study was supported by National Key Research and Development Program of China (2023YFE0202200, 2021YFA0910000), National Natural Science Foundation of China (32170985, 81771293, 32200785), Guangdong Province Basic and Applied Basic Research Grant (2021A1515110237, 2021B1515120089), Shenzhen Science and Technology Program (JCYJ20210324115800003, JCYJ20200109114608075), International collaboration project of Chinese Academy of Sciences (172644KYSB20200045), CAS-Croucher Funding Scheme for Joint Laboratories, and Guangdong Innovation Platform of Translational Research for Cerebrovascular Diseases. The funders were not involved in study design, data collection, data analysis, manuscript preparation and/or publication decisions.

Data availability

No datasets were generated or analysed during the current study.

Declarations

Ethics approval and consent to participate

All animal work was approved by the Institutional Animal Care and Use Committee of Shenzhen Institute of Advanced Technology, Chinese Academy of Sciences.

Consent for publication

All authors agreed on the content of this manuscript before its submission.

Competing interests

The authors declare no competing interests.

Received: 19 June 2024 / Accepted: 10 October 2024
Published online: 19 October 2024

References

1. Rudd KE, Johnson SC, Agesa KM, Shackelford KA, Tsoi D, Kievlan DR, et al. Global, regional, and national sepsis incidence and mortality, 1990–2017: analysis for the global burden of Disease Study. Lancet. 2020;395(10219):200–11.
2. Niederman MS, Baron RM, Bouadma L, Calandra T, Daneman N, DeWaele J, et al. Initial antimicrobial management of sepsis. Crit Care. 2021;25(1):307.
3. Kellum JA, Ronco C. The role of endotoxin in septic shock. Crit Care. 2023;27(1):400.
4. Gofton TE, Young GB. Sepsis-associated encephalopathy. Nat Rev Neurol. 2012;8(10):557–66.
5. Sonneville R, de Montmollin E, Poujade J, Garrouste-Orgeas M, Souweine B, Darmon M, et al. Potentially modifiable factors contributing to sepsis-associated encephalopathy. Intensive Care Med. 2017;43(8):1075–84.
6. Iwashyna TJ, Ely EW, Smith DM, Langa KM. Long-term cognitive impairment and functional disability among survivors of severe Sepsis. Jama-J Am Med Assoc. 2010;304(16):1787–94.
7. Zhang YY, Ning BT. Signaling pathways and intervention therapies in sepsis. Signal Transduct Target Ther. 2021;6(1):407.
8. Ji MH, Gao YZ, Shi CN, Wu XM, Yang JJ. Acute and long-term cognitive impairment following sepsis: mechanism and prevention. Expert Rev Neurother. 2023;23(10):931–43.
9. Hong Y, Chen P, Gao J, Lin Y, Chen L, Shang X. Sepsis-associated encephalopathy: from pathophysiology to clinical management. Int Immunopharmacol. 2023;124:110800. Pt A).
10. Profaci CP, Munji RN, Pulido RS, Daneman R. The blood-brain barrier in health and disease: important unanswered questions. J Exp Med. 2020;217(4).
11. Sweeney MD, Zhao Z, Montagne A, Nelson AR, Zlokovic BV. Blood-brain barrier: from physiology to Disease and back. Physiol Rev. 2019;99(1):21–78.
12. Huang X, Hussain B, Chang J. Peripheral inflammation and blood-brain barrier disruption: effects and mechanisms. CNS Neurosci Ther. 2021;27(1):36–47.
13. Erikson K, Tuominen H, Vakkala M, Liisanantti JH, Karttunen T, Syrjala H, et al. Brain tight junction protein expression in sepsis in an autopsy series. Crit Care. 2020;24(1):385.
14. Daneman R, Agalliu D, Zhou L, Kuhnert F, Kuo CJ, Barres BA. Wnt/beta-catenin signaling is required for CNS, but not non-CNS, angiogenesis. Proc Natl Acad Sci U S A. 2009;106(2):641–6.
15. Liebner S, Corada M, Bangsow T, Babbage J, Taddei A, Czupalla CJ, et al. Wnt/beta-catenin signaling controls development of the blood-brain barrier. J Cell Biol. 2008;183(3):409–17.

16. Stenman JM, Rajagopal J, Carroll TJ, Ishibashi M, McMahon J, McMahon AP. Canonical wnt signaling regulates organ-specific assembly and differentiation of CNS vasculature. Science. 2008;322(5905):1247–50.
17. Kuhnert F, Mancuso MR, Shamloo A, Wang HT, Choksi V, Florek M, et al. Essential regulation of CNS angiogenesis by the orphan G protein-coupled receptor GPR124. Science. 2010;330(6006):985–9.
18. Cullen M, Elzarrad MK, Seaman S, Zudaire E, Stevens J, Yang MY, et al. GPR124, an orphan G protein-coupled receptor, is required for CNS-specific vascularization and establishment of the blood-brain barrier. Proc Natl Acad Sci U S A. 2011;108(14):5759–64.
19. Wang Y, Rattner A, Zhou Y, Williams J, Smallwood PM, Nathans J. Norrin/Frizzled4 signaling in retinal vascular development and blood brain barrier plasticity. Cell. 2012;151(6):1332–44.
20. Zhou Y, Wang Y, Tischfield M, Williams J, Smallwood PM, Rattner A, et al. Canonical WNT signaling components in vascular development and barrier formation. J Clin Invest. 2014;124(9):3825–46.
21. Tran KA, Zhang X, Predescu D, Huang X, Machado RF, Gothert JR, et al. Endothelial beta-catenin signaling is required for maintaining adult blood-brain Barrier Integrity and Central Nervous System Homeostasis. Circulation. 2016;133(2):177–86.
22. Corada M, Orsenigo F, Bhat GP, Conze LL, Breviario F, Cunha SI, et al. Fine-tuning of Sox17 and canonical wnt coordinates the Permeability properties of the blood-brain barrier. Circ Res. 2019;124(4):511–25.
23. Ben-Zvi A, Lacoste B, Kur E, Andreone BJ, Mayshar Y, Yan H, et al. Mfsd2a is critical for the formation and function of the blood-brain barrier. Nature. 2014;509(7501):507–11.
24. Andreone BJ, Chow BW, Tata A, Lacoste B, Ben-Zvi A, Bullock K, et al. Blood-brain barrier permeability is regulated by lipid transport-dependent suppression of Caveolae-Mediated Transcytosis. Neuron. 2017;94(3):581–94. e5.
25. Hussain B, Fang C, Huang X, Feng Z, Yao Y, Wang Y, et al. Endothelial beta-catenin Deficiency causes blood-brain barrier breakdown via enhancing the Paracellular and transcellular permeability. Front Mol Neurosci. 2022;15:895429.
26. Wang Z, Liu CH, Huang S, Fu Z, Tomita Y, Britton WR, et al. Wnt signaling activates MFSD2A to suppress vascular endothelial transcytosis and maintain blood-retinal barrier. Sci Adv. 2020;6(35):eaba7457.
27. Chang J, Mancuso MR, Maier C, Liang X, Yuki K, Yang L, et al. Gpr124 is essential for blood-brain barrier integrity in central nervous system disease. Nat Med. 2017;23(4):450–60.
28. Ta S, Rong X, Guo ZN, Jin H, Zhang P, Li F, et al. Variants of WNT7A and GPR124 are associated with hemorrhagic transformation following intravenous thrombolysis in ischemic stroke. CNS Neurosci Ther. 2021;27(1):71–81.
29. Ji YB, Wang TX, Gao Q, Huang XW, Chang J. Normalization of non-canonical wnt signalings does not compromise blood-brain barrier protection conferred by upregulating endothelial Wnt/beta-catenin signaling following ischemic stroke. CNS Neurosci Ther. 2021;27(9):1085–96.
30. Ji YB, Gao Q, Tan XX, Huang XW, Ma YZ, Fang C, et al. Lithium alleviates blood-brain barrier breakdown after cerebral ischemia and reperfusion by upregulating endothelial Wnt/beta-catenin signaling in mice. Neuropharmacology. 2021;186:108474.
31. Reis M, Czupalla CJ, Ziegler N, Devraj K, Zinke J, Seidel S, et al. Endothelial Wnt/beta-catenin signaling inhibits glioma angiogenesis and normalizes tumor blood vessels by inducing PDGF-B expression. J Exp Med. 2012;209(9):1611–27.
32. Lengfeld JE, Lutz SE, Smith JR, Diaconu C, Scott C, Kofman SB, et al. Endothelial Wnt/beta-catenin signaling reduces immune cell infiltration in multiple sclerosis. Proc Natl Acad Sci U S A. 2017;114(7):E1168–77.
33. Niu J, Tsai HH, Hoi KK, Huang N, Yu G, Kim K, et al. Aberrant oligodendroglial-vascular interactions disrupt the blood-brain barrier, triggering CNS inflammation. Nat Neurosci. 2019;22(5):709–18.
34. Wang Q, Huang X, Su Y, Yin G, Wang S, Yu B et al. Activation of Wnt/beta-catenin pathway mitigates blood-brain barrier dysfunction in Alzheimer's disease. Brain. 2022.
35. Martin M, Vermeiren S, Bostaille N, Eubelen M, Spitzer D, Vermeersch M, et al. Engineered wnt ligands enable blood-brain barrier repair in neurological disorders. Science. 2022;375(6582):eabm4459.
36. Ding J, Lee SJ, Vlahos L, Yuki K, Rada CC, van Unen V, et al. Therapeutic blood-brain barrier modulation and stroke treatment by a bioengineered FZD(4)-selective WNT surrogate in mice. Nat Commun. 2023;14(1):2947.
37. Medeiros M, Candido MF, Valera ET, Brassesco MS. The multifaceted NF-kB: are there still prospects of its inhibition for clinical intervention in pediatric central nervous system tumors? Cellular and molecular life sciences. CMLS. 2021;78(17–18):6161–200.
38. Yu H, Lin LB, Zhang ZQ, Zhang HY, Hu HB. Targeting NF-kappa B pathway for the therapy of diseases: mechanism and clinical study. Signal Transduct Tar. 2020;5(1).
39. Ma B, Hottiger MO. Crosstalk between Wnt/beta-Catenin and NF-kappaB signaling pathway during inflammation. Front Immunol. 2016;7:378.
40. Cho HH, Song JS, Yu JM, Yu SS, Choi SJ, Kim DH, et al. Differential effect of NF-kappaB activity on beta-catenin/Tcf pathway in various cancer cells. FEBS Lett. 2008;582(5):616–22.
41. Pei J, Fan L, Nan K, Li J, Shi Z, Dang X, et al. Excessive activation of TLR4/NF-kappaB interactively suppresses the canonical Wnt/beta-catenin pathway and induces SANFH in SD rats. Sci Rep. 2017;7(1):11928.
42. Guan X, He Y, Wei Z, Shi C, Li Y, Zhao R, et al. Crosstalk between Wnt/beta-catenin signaling and NF-kappaB signaling contributes to apical periodontitis. Int Immunopharmacol. 2021;98:107843.
43. Jang J, Song J, Lee H, Sim I, Kwon YV, Jho EH, et al. LGK974 suppresses lipopolysaccharide-induced endotoxemia in mice by modulating the crosstalk between the Wnt/beta-catenin and NF-kappaB pathways. Exp Mol Med. 2021;53(3):407–21.
44. Jang J, Song J, Sim I, Kwon YV, Yoon Y. Wnt-signaling inhibitor Wnt-C59 suppresses the Cytokine Upregulation in multiple organs of Lipopolysaccharide-Induced Endotoxemic mice via reducing the Interaction between beta-catenin and NF-kappaB. Int J Mol Sci. 2021;22(12).
45. Harada N, Tamai Y, Ishikawa T, Sauer B, Takaku K, Oshima M, et al. Intestinal polyposis in mice with a dominant stable mutation of the beta-catenin gene. EMBO J. 1999;18(21):5931–42.
46. Wang Y, Nakayama M, Pitulescu ME, Schmidt TS, Bochenek ML, Sakakibara A, et al. Ephrin-B2 controls VEGF-induced angiogenesis and lymphangiogenesis. Nature. 2010;465(7297):483–6.
47. Yu M, Nie Y, Yang J, Yang S, Li R, Rao V, et al. Integrative multi-omic profiling of adult mouse brain endothelial cells and potential implications in Alzheimer's disease. Cell Rep. 2023;42(11):113392.
48. Nishioku T, Dohgu S, Takata F, Eto T, Ishikawa N, Kodama KB, et al. Detachment of brain pericytes from the basal lamina is involved in disruption of the blood-brain barrier caused by lipopolysaccharide-induced sepsis in mice. Cell Mol Neurobiol. 2009;29(3):309–16.
49. Banks WA, Gray AM, Erickson MA, Salameh TS, Damodarasamy M, Sheibani N, et al. Lipopolysaccharide-induced blood-brain barrier disruption: roles of cyclooxygenase, oxidative stress, neuroinflammation, and elements of the neurovascular unit. J Neuroinflammation. 2015;12:223.
50. Maggioli E, McArthur S, Mauro C, Kieswich J, Kusters DHM, Reutelingsperger CPM, et al. Estrogen protects the blood-brain barrier from inflammation-induced disruption and increased lymphocyte trafficking. Brain Behav Immun. 2016;51:212–22.
51. van Peters AM, Leijte GP, Franssen GM, Bruse N, Booij J, Doorduin J, et al. Human in vivo neuroimaging to detect reprogramming of the cerebral immune response following repeated systemic inflammation. Brain Behav Immun. 2021;95:321–9.
52. Zhao J, Bi W, Xiao S, Lan X, Cheng X, Zhang J, et al. Neuroinflammation induced by lipopolysaccharide causes cognitive impairment in mice. Sci Rep. 2019;9(1):5790.
53. Nusse R, Clevers H. Wnt/beta-Catenin signaling, Disease, and emerging therapeutic modalities. Cell. 2017;169(6):985–99.
54. Wang Y, Sabbagh MF, Gu X, Rattner A, Williams J, Nathans J. Beta-catenin signaling regulates barrier-specific gene expression in circumventricular organ and ocular vasculatures. Elife. 2019;8.
55. Qin K, Yu M, Fan J, Wang H, Zhao P, Zhao G, et al. Canonical and noncanonical wnt signaling: multilayered mediators, signaling mechanisms and major signaling crosstalk. Genes Dis. 2024;11(1):103–34.
56. Lamberti C, Lin KM, Yamamoto Y, Verma U, Verma IM, Byers S, et al. Regulation of beta-catenin function by the IkappaB kinases. J Biol Chem. 2001;276(45):42276–86.
57. Pierce JW, Schoenleber R, Jesmok G, Best J, Moore SA, Collins T, et al. Novel inhibitors of cytokine-induced IkappaBalpha phosphorylation and endothelial cell adhesion molecule expression show anti-inflammatory effects in vivo. J Biol Chem. 1997;272(34):21096–103.
58. Kodama Y, Hu CD. Bimolecular fluorescence complementation (BiFC): a 5-year update and future perspectives. Biotechniques. 2012;53(5):285–98.
59. Milstone DS, Ilyama M, Chen M, O'Donnell P, Davis VM, Plutzky J, et al. Differential role of an NF-kappaB transcriptional response element in endothelial versus intimal cell VCAM-1 expression. Circ Res. 2015;117(2):166–77.

60. Zhou Y, Nathans J. Gpr124 controls CNS angiogenesis and blood-brain barrier integrity by promoting ligand-specific canonical wnt signaling. Dev Cell. 2014;31(2):248–56.
61. Posokhova E, Shukla A, Seaman S, Volate S, Hilton MB, Wu B, et al. GPR124 functions as a WNT7-specific coactivator of canonical beta-catenin signaling. Cell Rep. 2015;10(2):123–30.
62. Eubelen M, Bostaille N, Cabochette P, Gauquier A, Tebabi P, Dumitru AC, et al. A molecular mechanism for wnt ligand-specific signaling. Science. 2018;361(6403):1–13.
63. Hussain B, Fang C, Huang X, Feng Z, Yao Y, Wang Y et al. Endothelial β-Catenin Deficiency causes blood-brain barrier breakdown via enhancing the Paracellular and transcellular permeability. Front Mol Neurosci. 2022;15.
64. Chen MB, Yang AC, Yousef H, Lee D, Chen W, Schaum N, et al. Brain endothelial cells are exquisite sensors of age-related circulatory cues. Cell Rep. 2020;30(13):4418–32. e4.
65. Flierl MA, Stahel PF, Rittirsch D, Huber-Lang M, Niederbichler AD, Hoesel LM et al. Inhibition of complement C5a prevents breakdown of the blood-brain barrier and pituitary dysfunction in experimental sepsis. Crit Care. 2009;13(1).
66. Daneman R, Agalliu D, Zhou L, Kuhnert F, Kuo CJ, Barres BA. Wnt/β-catenin signaling is required for CNS, but not non-CNS, angiogenesis. P Natl Acad Sci USA. 2009;106(2):641–6.
67. Guérit S, Fidan E, Macas J, Czupalla CJ, Figueiredo R, Vijikumar A et al. Astrocyte-derived wnt growth factors are required for endothelial blood-brain barrier maintenance. Prog Neurobiol. 2021;199.
68. Boyé K, Geraldo LH, Furtado J, Pibouin-Fragner L, Poulet M, Kim D et al. Endothelial Unc5B controls blood-brain barrier integrity. Nat Commun. 2022;13(1).
69. Song DP, Ji YB, Huang XW, Ma YZ, Fang C, Qiu LH, et al. Lithium attenuates blood-brain barrier damage and brain edema following intracerebral hemorrhage via an endothelial Wnt/beta-catenin signaling-dependent mechanism in mice. Cns Neurosci Ther. 2022;28(6):862–72.
70. Ji YB, Gao Q, Tan XX, Huang XW, Ma YZ, Fang C et al. Lithium alleviates blood-brain barrier breakdown after cerebral ischemia and reperfusion by upregulating endothelial Wnt/β-catenin signaling in mice. Neuropharmacology. 2021;186.
71. Lei S, Li J, Yu JJ, Li FL, Pan YP, Chen X et al. Bacteremia increases the permeability of the blood-brain barrier via the Mfsd2a/Caveolin-1 mediated transcytosis pathway. Int J Oral Sci. 2023;15(1).
72. Ayloo S, Gu CH. Transcytosis at the blood-brain barrier. Curr Opin Neurobiol. 2019;57:32–8.
73. Andreone BJ, Chow BW, Tata A, Lacoste B, Ben-Zvi A, Bullock K, et al. Blood-brain barrier permeability is regulated by lipid transport-dependent suppression of Caveolae-Mediated Transcytosis. Neuron. 2017;94(3):581–.
74. Ryu JK, Kim SJ, Rah SH, Kang JI, Jung HE, Lee D, et al. Reconstruction of LPS transfer Cascade reveals structural determinants within LBP, CD14, and TLR4-MD2 for efficient LPS recognition and transfer. Immunity. 2017;46(1):38–50.
75. Hailman E, Lichenstein HS, Wurfel MM, Miller DS, Johnson DA, Kelley M, et al. Lipopolysaccharide (LPS)-binding protein accelerates the binding of LPS to CD14. J Exp Med. 1994;179(1):269–77.
76. Shi J, Zhao Y, Wang Y, Gao W, Ding J, Li P, et al. Inflammatory caspases are innate immune receptors for intracellular LPS. Nature. 2014;514(7521):187–92.
77. Vasudevan SO, Russo AJ, Kumari P, Vanaja SK, Rathinam VA. A TLR4-independent critical role for CD14 in intracellular LPS sensing. Cell Rep. 2022;39(5):110755.
78. Yousef H, Czupalla CJ, Lee D, Chen MB, Burke AN, Zera KA, et al. Aged blood impairs hippocampal neural precursor activity and activates microglia via brain endothelial cell VCAM1. Nat Med. 2019;25(6):988–1000.
79. Conlon TM, John-Schuster G, Heide D, Pfister D, Lehmann M, Hu Y, et al. Inhibition of LTβR signalling activates WNT-induced regeneration in lung. Nature. 2020;588(7836):151–.
80. Pei JP, Fan LH, Nan K, Li J, Shi ZB, Dang XQ et al. Excessive activation of TLR4/NF-κB interactively suppresses the canonical Wnt/β-catenin pathway and induces SANFH in SD rats. Sci Rep-Uk. 2017;7.
81. Guan XY, He YN, Wei ZC, Shi C, Li YX, Zhao R et al. Crosstalk between Wnt/β-catenin signaling and NF-κB signaling contributes to apical periodontitis. Int Immunopharmacol. 2021;98.
82. Audrey R, Fetsko DJS, Lilyana B, Budzynski A, Scharbarth MR, Taylor. IL-1β disrupts the initiation of blood-brain barrier development by inhibiting endothelial Wnt/β-catenin signaling. iScience. 2024;25(5):18.
83. Deng JO, Miller SA, Wang HY, Xia WY, Wen Y, Zhou BHP, et al. β-catenin interacts with and inhibits NF-κB in human colon and breast cancer. Cancer Cell. 2002;2(4):323–34.
84. Nusse R, Clevers H. Wnt/β-Catenin signaling, Disease, and emerging therapeutic modalities. Cell. 2017;169(6):985–99.
85. Daugherty RL, Gottardi CJ. Phospho-regulation of β-catenin adhesion and signaling functions. Physiology. 2007;22(5):303–9.
86. Farooq M, Kim S, Patel S, Khatri L, Hikima T, Rice ME, et al. Lithium increases synaptic GluA2 in hippocampal neurons by elevating the δ-catenin protein. Neuropharmacology. 2017;113:426–33.
87. Qudus MS, Tian MF, Sirajuddin S, Liu SY, Afaq U, Wali M et al. The roles of critical pro-inflammatory cytokines in the drive of cytokine storm during SARS-CoV-2 infection. J Med Virol. 2023;95(4).
88. Jamil Al-Obaidi MM, Desa MNM. A review of the mechanisms of blood-brain barrier disruption during COVID-19 infection. J Neurosci Res. 2023.
89. Yamada S, Hashita T, Yanagida S, Sato H, Yasuhiko Y, Okabe K, et al. SARS-CoV-2 causes dysfunction in human iPSC-derived brain microvascular endothelial cells potentially by modulating the wnt signaling pathway. Fluids Barriers CNS. 2024;21(1):32.
90. Trevino TN, Fogel AB, Otkiran G, Niladhuri SB, Sanborn MA, Class J et al. Engineered Wnt7a ligands rescue blood-brain barrier and cognitive deficits in a COVID-19 mouse model. Brain. 2024.
91. Gust J, Hay KA, Hanafi LA, Li D, Myerson D, Gonzalez-Cuyar LF, et al. Endothelial activation and blood-brain barrier disruption in neurotoxicity after adoptive immunotherapy with CD19 CAR-T cells. Cancer Discov. 2017;7(12):1404–19.
92. Segura-Collar B, Mata-Martinez P, Hernandez-Lain A, Sanchez-Gomez P, Gargini R. Blood-brain barrier disruption: a common driver of Central Nervous System diseases. Neuroscientist. 2022;28(3):222–37.
93. Wei C, Jiang W, Wang R, Zhong H, He H, Gao X et al. Brain endothelial GSDMD activation mediates inflammatory BBB breakdown. Nature. 2024.

Publisher's note

Springer Nature remains neutral with regard to jurisdictional claims in published maps and institutional affiliations.